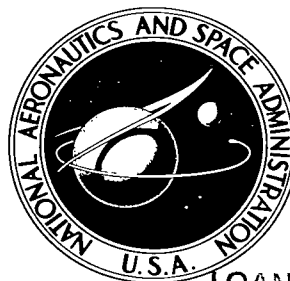


NASA TECHNICAL NOTE



NASA TN D-4104

a.1

NASA TN D-4104

LOAN COPY: RETURN TO
AFWL (WLIL-2)
KIRTLAND AFB, N MEX



**LOW-THRUST ORBIT RAISING IN
CONTINUOUS SUNLIGHT WHILE THRUSTING
IN A PLANE PERPENDICULAR
TO THE EARTH-SUN LINE**

by James R. Ramler

Lewis Research Center

Cleveland, Ohio



LOW-THRUST ORBIT RAISING IN CONTINUOUS SUNLIGHT
WHILE THRUSTING IN A PLANE PERPENDICULAR
TO THE EARTH-SUN LINE

By James R. Ramler

Lewis Research Center
Cleveland, Ohio

NATIONAL AERONAUTICS AND SPACE ADMINISTRATION

For sale by the Clearinghouse for Federal Scientific and Technical Information
Springfield, Virginia 22151 - CFSTI price \$3.00

LOW-THRUST ORBIT RAISING IN CONTINUOUS SUNLIGHT WHILE THRUSTING IN A PLANE PERPENDICULAR TO THE EARTH-SUN LINE

by James R. Ramler
Lewis Research Center

SUMMARY

An approximate numerical method is derived for determining the motion of an Earth satellite following a tightly wound, spiral trajectory which is nearly circular at all times while remaining in continuous sunlight. Thrust is provided by electric rockets and is continuous, tangential, and in a plane perpendicular to the Earth-Sun line. This differs from previous studies which have generally assumed the thrust vector to lie in the orbit plane. The maximum time that the satellite can remain in continuous sunlight has been computed by optimizing the initial orbit inclination and mission starting time for initial thrust-weight ratios from 2.5×10^{-6} to 8.0×10^{-6} and initial orbit altitudes of 300, 500, and 800 nautical miles (555.6, 926.0, and 1481.6 km). Precession of the orbital plane is largely accomplished by utilizing the effects of the oblateness of the Earth. The effect of reversing the thrust direction during the latter part of the mission on the maximum time spent in continuous sunlight has been studied. Methods of solution are discussed and results are presented as curves. Errors in establishing the required initial orbit conditions inherent in any realistic satellite launching are briefly discussed.

INTRODUCTION

Testing of electric rockets in an actual space environment will be required to demonstrate fully their performance characteristics, in particular, their operation lifetime. The operating lifetime of electric rockets may be demonstrated in an actual space environment by continuously operating them for a long period of time in orbit about the earth. While a number of trajectory concepts may be envisioned, the purpose of this report is to analyze one of them - that of raising the orbit altitude by thrusting tangentially,

thus enabling an accurate determination of the thrust level from orbit mechanics. Changing the orbit altitude by thrusting tangentially would also demonstrate the capability of electric rockets to perform useful missions in the future.

Such a mission would require continuous electric power to be supplied to the electric thrusters for a long period of time. The most likely source of power for this, as well as similar missions in the near future, is solar cells which are lightweight and can operate for long durations. In order to demonstrate the operating lifetime of electric rockets, it will be desirable to keep the satellite with its solar cells in continuous sunlight as long as possible.

For an Earth satellite to remain in continuous sunlight as long as possible, its orbit must be near polar and the orbit plane must be rotated with time in an easterly direction. This will tend to keep the Sun in a direction normal to the orbit plane, thus continuously illuminating the satellite as the Sun changes position in its apparent motion along the ecliptic during the year. This orbit rotation or precession can be accomplished by utilizing the effects of the oblateness of the Earth on an inclined orbit (ref. 1).

The problem of raising the orbit of a satellite using low thrust while remaining in continuous sunlight has been studied in reference 2. Altitude raising was accomplished by using a continuous tangential thrust in the orbit plane starting from a low circular Earth orbit. The maximum final altitude or mission time which could be reached was computed by an approximate technique. The effects of initial orbit and mission parameters such as inclination, altitude, thrust-weight ratio, and mission starting time were studied.

Tangential thrusting in the orbit plane has been shown to be an efficient steering program for orbit raising (ref. 3). However, if the solar panels are oriented to always face the sun, tangential thrusting in the orbit plane introduces several complications into the spacecraft design. For example, the thrusters must be gimballed with respect to the solar panels and a cyclic variation in gimbal angle is required during each orbit revolution. The maximum total gimbal angle (equivalent to η) can become as high as $\pm 70^\circ$ as shown in reference 2 (all symbols are defined in appendix A). Furthermore, the inertial direction of motion of the satellite must be continuously determined onboard the satellite in order to thrust in the orbit plane.

For this study, a steering concept was assumed that would be simpler to implement although somewhat less efficient than tangential thrusting. It is based on a conceptual design in which the solar panels and electric thrusters would be rigidly fixed to the spacecraft frame (except for possibly a small gimbaling capability on the thrusters for attitude control). The solar panel and thrust vector geometry will be discussed in more detail later. Briefly, however, the spacecraft would be oriented so that the solar cell panels always face the sun. The panels would, therefore, lie in a plane perpendicular to the Earth-Sun line. The electric thrusters would lie in the same plane as the solar

panels and, in addition, would be oriented to always thrust in the local horizontal plane. This geometry will result in a variable component of thrust normal to the orbit plane.

This study then considered the case of an Earth satellite using electric rockets that thrust tangentially in a plane perpendicular to the Earth-Sun line rather than thrusting tangentially in the orbit plane as was the case in reference 2. This steering concept could be implemented using only horizon scanners and Sun seekers.

The thrust vector can be considered to have two components: one in the orbit plane and the other normal to the orbit plane. An approximate numerical solution has been derived to determine the motion of an Earth satellite under these conditions while remaining in continuous sunlight. Although this solution was derived to analyze the effect of a normal component of thrust resulting from a particular orientation of the satellite with respect to the orbit plane and the Sun, the approach to the problem and method of solution presented in this report would be generally applicable to other low-thrust, circular Earth orbit missions having out-of-plane thrusting. The mathematical analysis for this study is presented in appendix B.

By use of the results of appendix B, the maximum time that an Earth satellite can remain in continuous sunlight was computed by optimizing the initial orbit and mission variables and by utilizing the oblateness of the Earth as the major orbital-plane rotation mechanism. The ranges of initial variables investigated parametrically included orbit altitudes of 300, 500, and 800 nautical miles (555.6, 926.0, and 1481.6 km), thrust-weight ratios from 2.5×10^{-6} to 8.0×10^{-6} and mission starting dates throughout the year. Initial orbit inclination and the time of day at the start of the mission were optimized for each point. The effect of reversing the thrust of the satellite during the latter part of the mission was studied in an attempt to extend the maximum time that the satellite remains in continuous sunlight. This reversal would be effected by simply pitching the spacecraft over 180° . The time of thrust reversal was optimized for each case.

For comparison, the case where thrusting is completely tangential and in the orbit plane was also investigated, thus extending the results of reference 2 to lower values of thrust-weight ratios.

Errors in establishing the required initial orbit conditions inherent in any realistic satellite launching and their effect on the mission are briefly discussed.

ANALYSIS

Thrust Vector Geometry

Consider the spacecraft shown in figure 1 to be in a near polar circular Earth orbit. For a satellite orbiting the Earth using continuous low thrust, tangential thrusting has

been shown to be nearly the most efficient for increasing energy (ref. 3). As seen in figure 1, tangential thrusting in a circular orbit can be obtained by simply keeping the roll axis of the spacecraft parallel to the local horizontal plane. In addition, the solar cell panels would be oriented to face the Sun by aligning the pitch axis of the spacecraft toward the Sun. This will keep the solar cell panels normal to the incident radiation of the Sun, thus taking full advantage of their energy conversion efficiency.

To keep the roll axis of the satellite parallel to the local horizontal plane as it orbits the Earth, it would be necessary to control the attitude of the satellite in pitch. Also, to keep the pitch axis of the satellite pointed toward the Sun, it would be necessary to control the attitude of the satellite in roll and yaw. Rolling of the satellite will have no effect on the thrust vector; whereas, yawing will cause it to move out of the orbit plane. With the roll axis maintained parallel to the local horizontal plane, however, yawing will only result in a component of thrust normal to the orbit plane (the in-plane component remains tangential). For this study, then, the thrust vector consists of two variable components; one tangential and in the orbit plane and the other normal to the orbit plane. This thrust vector alignment may not necessarily be optimum, but, for early research and development flights, it would provide an effective steering program that could be implemented by using horizon scanners and Sun seekers.

With the attitude of the satellite determined as described previously, the thrust acceleration vector A will always be tangential and lie parallel to a plane perpendicular to the sunline as shown in figure 2. For simplicity, the sunline is defined as a vector from the center of the Earth to the center of the Sun, rather than from the spacecraft to the Sun; thus, a very small error in angle between the orbit plane and the pitch axis of the spacecraft (less than 0.01° for orbit altitudes up to 10 000 n mi (18 520 km)) is neglected. As illustrated in figure 2, attitude changes of the spacecraft can be assumed to be periodic over one orbit if the inertial positions of the orbit plane and the Sun are assumed not to change during one orbit. This is a good assumption for one or even several orbits since the relative motion of the Sun and the orbit plane will be very slow. Because the thrusters are fixed parallel to the roll axis of the spacecraft, the thrust acceleration vector A will then also periodically change direction with respect to the orbit plane over one orbit. As illustrated in figure 2, it can be seen that, in the orbital positions 1 and 3, the orbit track and the plane perpendicular to the sunline intersect. When the spacecraft is at these positions, the yaw axis will be aligned with the radius vector so that there is no displacement in roll. However, there will be a yaw angle at positions 1 and 3 equal to the angle η between the orbit plane and the plane perpendicular to the sunline. This will result in a component of thrust acceleration W normal to the orbit plane at these positions. At positions 2 and 4, which are displaced 90° from positions 1 and 3, there will be no displacement in yaw but in roll. At these positions, the normal component of acceleration will be zero and the total thrust acceleration A will be tangential in the plane of the

orbit. From the analysis in appendix B, it is shown that the magnitude of the normal component of thrust acceleration W will vary periodically over one orbit from zero at positions 2 and 4 to a maximum equal to $A \sin \eta$ at positions 1 and 3. Likewise, the magnitude of the tangential component of thrust acceleration C will vary from a minimum equal to $A \cos \eta$ at positions 1 and 3 to a maximum equal to the total thrust acceleration A at positions 2 and 4.

The acceleration components, W and C , will also vary secularly with time. Although it was assumed that the inertial positions of the Sun and the orbit plane do not change during one orbit or even during several orbits, they actually do change continuously with time; that is, the angle η between the orbit plane and the plane perpendicular to the sunline will vary continuously with time. The variation of η depends on the motion of the Sun in right ascension and declination and the changes in inclination and nodal position of the orbit plane. Changes in the inclination and node of the orbit plane are caused by perturbations due to the oblateness of the Earth, thrust of the spacecraft, and other bodies such as the Sun and Moon.

Orbit Perturbations

The forces on a satellite in a circular Earth orbit due to oblateness will cause the orbit plane to precess about the polar axis of the Earth. An analytical expression for the secular rate of change of nodes of an orbit can be obtained by considering only the terms through the second harmonic in the potential function of the oblate Earth. The following expression is obtained in reference 4 by ignoring the smaller, higher order terms in the potential function:

$$\dot{\Omega} \approx -\sqrt{\mu} J R_E^2 (R_E + h)^{-7/2} \cos I \quad \text{for } 0^\circ \leq I \leq 180^\circ \quad (1)$$

where J is the coefficient of the second harmonic in the gravitational potential function. Note that, for inclinations greater than 90° (retrograde orbits), $\dot{\Omega}$ is positive, which results in an eastward precession of the node. This is the desired precession direction to keep the Sun in a proper position relative to the orbit plane. All the orbits studied, therefore, have inclinations greater than 90° . Perturbations due to the oblateness of the Earth of other orbital elements such as inclination, eccentricity, and semimajor axis are small and periodic with no resultant secular change.

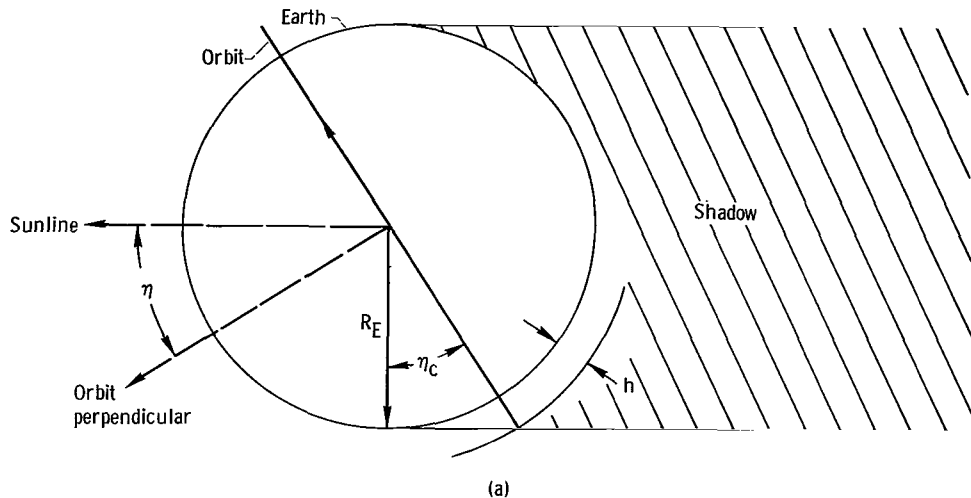
The normal component of thrust acceleration W causes secular variations in both $\dot{\Omega}$ and I which are given by equations (B12). Other orbital elements will exhibit only small periodic changes over one orbit but no secular changes because of the normal component of thrust acceleration. The tangential component of thrust acceleration C changes

only the orbit altitude. (Note that, for circular orbits, the tangential- and circumferential-thrust vector directions are identical.)

As is shown later, perturbations of the orbital elements due to the Sun and Moon were found to be negligible and are not included in the numerical approximation.

Earth Shadow Considerations

By assuming only circular orbits, the geometry of the orbit with respect to illumination from the Sun is simplified. The existence of a penumbra region of shadow is neglected and it is assumed that the rays of the Sun are parallel, causing a cylinder shaped umbra region behind the Earth. Shown in sketch (a) is an edgewise view of the orbit plane and its geometrical relation to the position of the Sun. The angle between the orbit perpendicular (orbital angular-velocity vector) and the sunline is defined as η . It can be seen from sketch (a) that as long as η is less than η_c , the entire orbit will be in sunlight. The situation depicted in sketch (a) is a limiting case in which the orbit is just on the edge of the cylindrical shadow and η equals η_c .



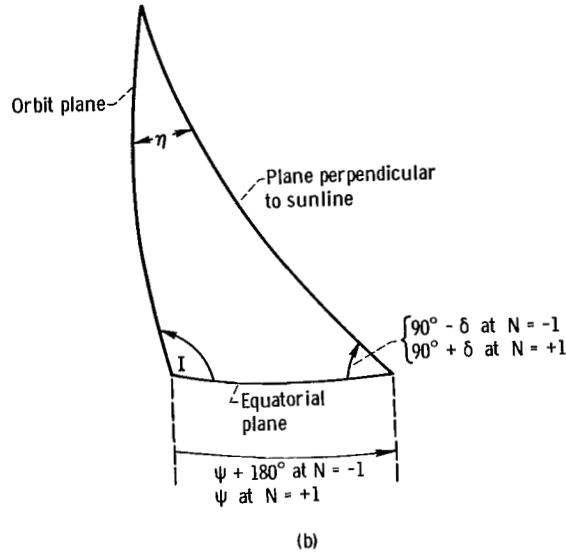
(The plane of the sketch is the plane containing the sunline and the orbit perpendicular.)
From sketch (a), η_c is defined by

$$\cos \eta_c = \frac{R_E}{R_E + h} \quad \text{for } 0^\circ < \eta_c < 90^\circ \quad (2)$$

This means that, for an orbit to be in continuous sunlight, the orbit perpendicular must remain inside a cone having the moving sunline as its axis. The half-angle of this cone

is the η_c corresponding to the instantaneous orbit altitude. This cone (fig. 3, taken from ref. 2) is called the cone of tolerance and the intersection of the cone of tolerance and the surface of the Earth is called the circle of tolerance.

An expression for the angle η can be derived from sketch (b).



Consider the spherical triangle formed by the orbit plane, the plane perpendicular to the sunline, and the equatorial plane. The angle η is the angle between the orbit plane and the plane perpendicular to the sunline. As seen in figure 3, the angle ψ is defined to be the difference between the right ascension of the Sun α and the position of the orbit perpendicular in longitude Ω . As such, it is an indication of how far the orbit perpendicular is west of (lagging behind) the easterly moving sunline. The orbit index, $N = +1$, corresponds to the sunline being on the same side of the orbit plane as the orbit perpendicular (orbital angular-velocity vector), and $N = -1$ corresponds to the sunline being on the opposite side of the orbit plane as the orbit perpendicular. It should be noted that for $N = -1$, ψ must be 180° larger than ψ for $N = +1$.

From sketch (b), for $N = -1$

$$\cos(\psi + 180^\circ) = \frac{\cos \eta + \cos I \cos(90^\circ - \delta)}{\sin I \sin(90^\circ - \delta)}$$

Therefore,

$$\cos \eta = -\cos \psi \sin I \cos \delta - \cos I \sin \delta$$

For $N = +1$

$$\cos \psi = \frac{\cos \eta + \cos I \cos(90^\circ + \delta)}{\sin I \sin(90^\circ + \delta)}$$

Therefore,

$$\cos \eta = \cos \psi \sin I \cos \delta + \cos I \sin \delta$$

and, in general,

$$\cos \eta = N(\cos \psi \sin I \cos \delta + \cos I \sin \delta) \quad (3)$$

The angle η can then be evaluated from equation (3) and compared with the angle η_c evaluated from equation (2) to determine whether or not the satellite orbit remains in sunlight.

Mechanics of Problem

During the mission, the orbit perpendicular will describe a path within the circle of tolerance. As long as this path remains within the circle of tolerance, the orbit will be in continuous sunlight. The problem can then be viewed as starting the mission with the orbit perpendicular inside the circle of tolerance and then maximizing the time that the orbit perpendicular remains within the circle of tolerance. Several factors will influence the motion of the orbit perpendicular within the circle of tolerance.

As the Earth moves about the Sun during the year, α and δ change continuously. Although α is an increasing function, δ varies between approximately 23.5° and -23.5° . Since the sunline is the axis of the cone of tolerance, as α changes, the cone of tolerance moves in longitude along the ecliptic. As δ changes, the cone of tolerance moves above and below the ecliptic in a periodic manner. Each location of the cone axis corresponds to a specific time of year.

Tangential thrust will cause the altitude of a circular orbit to increase (eq. (B13)). As the orbit altitude increases, the half-angle of the cone of tolerance η_c will also increase (eq. (2)) as the cone of tolerance moves along the ecliptic. In addition, as the orbit altitude increases, the precession rate due to oblateness decreases (eq. (1)).

Considering all these factors, therefore, it is evident that some relative motion exists between the orbit perpendicular and the sunline. This is illustrated in figure 4 where the orbit perpendicular is shown describing a path within the circle of tolerance.

The radius of the circle, which is η_c , is shown increasing with altitude and therefore with time.

An optimum mission (one which maximizes time in continuous sunlight) will typically start with the orbit perpendicular on the circle of tolerance at position 1 in figure 4. The initial inclination and altitude of the orbit are chosen such that the precession of the orbit plane, at first, will be faster than the movement of the Sun along the ecliptic. This causes the orbit perpendicular to move across the expanding circle along path a to position 2 where it just approaches the shadow line. At this position, the orbit altitude will have increased to the point where the decreased precession of the orbit plane is now nearly equal to the movement of the Sun along the ecliptic. Any further increase in altitude causes the orbit precession to become less than the angular rate of the Sun. This, in turn, causes the orbit perpendicular to return across the still expanding circle of tolerance until shadow is encountered at position 3.

For the range of thrust-weight ratios investigated, it was found that the maximum time in sunlight is attained when the orbit perpendicular initially starts as far behind the sunline as possible which means starting on the edge of the circle of tolerance (such as position 1 in fig. 4). Thus, ψ_0 is determined from equation (3) at the initial conditions.

$$\cos \psi_0 = \frac{\cos \eta_{c,0} - N \sin \delta_0 \cos I_0}{N \cos \delta_0 \sin I_0} \quad (4)$$

The angle ψ_0 , therefore, is a function of initial altitude, inclination, and mission starting date. For a given initial altitude, mission starting date, and thrust-weight ratio, the initial inclination must be optimized so that the orbit perpendicular will just approach the edge of the circle of tolerance at position 2 in figure 4. An inclination smaller than the optimum will cause the orbit perpendicular to follow path b which does not take full advantage of the expanding circle of tolerance, thereby reducing the time spent in continuous sunlight. An inclination greater than the optimum will cause the orbit perpendicular to follow path c resulting in a portion of the orbit entering shadow at position 2 on path c. Consequently, this will result in a much shorter time spent in continuous sunlight than either paths a or b.

Thrust Reversal

As discussed in the preceding section, as path a in figure 4 proceeds past position 2, the increasing altitude causes the orbit precession to become increasingly less than the angular rate of the Sun along the ecliptic. This causes the orbit perpendicular to return across the expanding circle of tolerance until, finally, shadow is encountered at posi-

tion 3. If, however, the orbit altitude is decreased during the latter portion of the mission starting at some point after position 2, the orbit precession can again be increased, thereby extending the time spent in continuous sunlight. This can be accomplished by simply reversing the thrust vector over the latter part of the mission, thereby reducing the altitude. Such a maneuver may be very useful for a development flight such as SERT where it is desirable to stay in continuous sunlight as long as possible.

The effect of thrust reversal is illustrated in figure 5. Without thrust reversal, the orbit perpendicular follows path a until shadow is encountered at position 3. With thrust reversal, the orbit perpendicular follows path a until the thrust is reversed and thereafter follows path b until it finally leaves the shrinking circle of tolerance at position 4. After thrust reversal, the altitude, and, therefore, the radius of the circle of tolerance, decreases until it is approximately equal to the initial altitude at position 4.

Methods of Computation

Precise solutions for the type of mission described in this report could be obtained by numerically integrating each orbit of the trajectory by using a computer code such as that described in reference 5. However, this is not a feasible approach for a parametric study requiring many solutions because of the computer time required. For example, the time for the N-Body code of reference 5 to integrate 1000 circular orbits is nearly an hour, and a typical mission consists of at least several thousand orbits.

Consequently, the approximate procedure developed in appendix B is very useful for obtaining a large number of solutions with a minimum of computation time. The equations derived in appendix B were programmed for solution on a high-speed digital computer. Computations were made basically at intervals of 10 orbits; that is, the change over one orbit of each of the variables of interest was computed at the beginning of an interval and simply multiplied by 10 to get the total change over the interval. Each variable was then updated. After investigating several computation intervals, the 10-orbit interval was chosen as a good compromise between computational accuracy and computer time required.

The computation of each solution consisted of choosing a specific starting date and initial inclination. The right ascension and declination of the Sun were obtained for any date and time by using the mean orbital elements of the solar ellipse with respect to the Earth from reference 5. The initial angle by which the orbit perpendicular lagged the sunline ψ_0 was determined from equation (4).

For a specific starting date, each initial inclination was checked to see how long the mission could proceed before the orbit entered shadow. This involved an orbit by orbit comparison of η and η_c as computed from equations (2) and (3). The inclination was

then iterated until the optimum value (corresponding to the maximum time in continuous sunlight) was found to within at least 0.01° . This process was then repeated for different mission starting dates until the optimum starting date was found.

For the cases where the thrust was reversed during the latter part of the mission, the optimum starting inclination was first determined by computing the mission with no thrust reversal as discussed previously. This same inclination then, proved to be the optimum when the thrust was reversed, since the optimum time of thrust reversal always occurred after the first close approach to the shadow line (position 2 in fig. 4). The time of thrust reversal was iterated until the optimum value was found. This same process was then repeated for different mission starting dates until the optimum starting date was obtained.

RESULTS AND DISCUSSION

Cases with no Thrust Reversal

Figure 6 shows the maximum durations spent in continuous sunlight, the corresponding final altitudes attained, the corresponding optimum mission starting dates, and initial inclinations required as functions of initial thrust-weight ratio. The initial altitudes are 300, 500, and 800 nautical miles (555.6, 926.0, and 1481.6 km). The results in figure 6 are presented for the case where the Sun is on the same side of the orbit plane as the orbit perpendicular (i. e., $N = +1$) and are characterized by mission starting dates in late summer and autumn. The solid curves are the results for thrusting tangentially in the plane perpendicular to the sunline. For comparison, the dashed curves display the results for thrusting tangentially in the orbit plane.

For the low thrust-weight ratios studied, thrusting in a plane perpendicular to the sunline and, therefore, out of the orbit plane has little effect on the mission duration when compared with the case of thrusting tangentially in the orbit plane. For example, in figure 5, note that the mission duration for an initial thrust-weight ratio of 5.0×10^{-6} and initial altitude of 500 nautical miles (926 km) would be 433 days for thrusting tangentially in a plane perpendicular to the sunline compared with 428 days for thrusting tangentially in the orbit plane. Also note from figure 5 for these two cases, there is little difference in either mission starting date or initial inclination. The required mission starting dates for these cases would be September 7 and September 9, respectively, and the required initial inclinations would be 107.5° and 107.9° , respectively. The greatest effect of thrusting out of the orbit plane is to reduce the final altitude achieved. This is because thrusting out of the orbit plane reduces the in-plane tangential component of thrust and, therefore, for a given mission duration, the final altitude attained will be less. In fig-

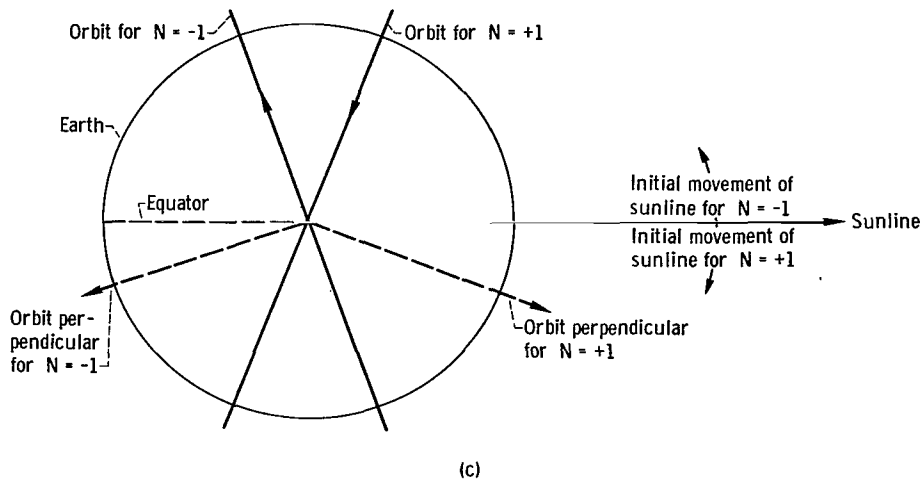
ure 6 for the sample cases, the final altitudes attained would be about 3150 and 3500 nautical miles (5833.8 and 6482.0 km), respectively.

The magnitude of the thrust component normal to the orbit plane may approach 90 percent of the total thrust near the end of the mission ($\eta \approx 60^\circ$). However, the effect of this normal component of thrust on nodal precession is at least an order of magnitude less than that due to the oblateness of the Earth and its cumulative effect on orbit inclination is to reduce the starting inclination only several degrees by the end of the mission. For higher thrust-weight ratios, of course, the effects of thrusting out of the orbit plane will be increasingly significant.

Shown in figure 7 is a typical variation of mission duration or time spent in continuous sunlight as a function of mission starting date. The curves shown are for an initial altitude of 500 nautical miles (926 km) and a thrust-weight ratio of 5.0×10^{-6} . Other altitude and thrust-weight ratio combinations would display similar trends, however. It should be noted that each point on these curves is fully optimized; that is, each has an optimum initial inclination and ψ_0 .

For any mission starting date, two solutions, $N = +1$ and $N = -1$, are possible so that the two curves shown in figure 7 are actually continuous and periodic. However, the lower portions of the curves representing solutions at unfavorable mission starting dates are not shown. The period from about mid-February to mid-August, for example, is unfavorable for $N = +1$ solutions. Favorable mission starting dates occur in the spring for $N = -1$ cases and in the late summer and autumn for $N = +1$ cases.

A qualitative understanding of why a particular mission starting date is more favorable than another may be had by considering the mean yearly variation of the declination of the Sun shown in figure 8 and the geometry of sketch (c). In sketch (c), are shown edgewise views of typical orbit planes for $N = +1$ and $N = -1$, each having an inclination greater than 90° . Also shown are the typical relative locations of the orbit perpendiculars and the sunline insofar as these are determined by inclination and declination at the beginning of the flight. In reality, the orbit perpendicular will generally not have the same longitude as the sunline. The sunline is shown in the equatorial plane with arrows indicating that it will move either above or below the equator as time progresses.



(The plane of the sketch is the plane containing the sunline and the orbit perpendicular.)

For an $N = +1$ case, the most favorable starting dates occur in the autumn such that, as time progresses, the Sun moves toward negative declinations. This tends to keep the Sun in the vicinity of the orbit perpendicular, thus illuminating the entire orbit for a longer period of time. This relative alignment is more important early in the mission, when the orbit altitude is small, than later in the mission, when the altitude is larger and a greater angle can be permitted between the Sun line and the orbit perpendicular. For an $N = -1$ case, the most favorable starting dates occur in the spring such that, as time progresses, the Sun moves toward positive declinations. Note that negative declinations are unfavorable for an $N = -1$ case.

Cases with Thrust Reversal

In figure 9 are shown the maximum durations spent in continuous sunlight and the corresponding maximum altitudes attained as functions of initial thrust-weight ratio with thrust reversal. Also shown in figure 9 are the optimum mission starting dates, initial inclinations, and thrust reversal times. The initial altitudes are 300, 500, and 800 nautical miles (555.6, 926.0, and 1481.6 km). The results are presented for $N = +1$ and for thrusting tangentially in a plane perpendicular to the sunline (solid curves) and thrusting tangentially in the orbit plane (dashed curves). Here again, as for the cases with no thrust reversal, thrusting out of the orbit plane has little effect on either mission starting date or initial inclination. The effects on thrust reversal time and maximum altitude attained are somewhat larger. The altitudes presented are maximum and not final, since, with thrust reversal, the final altitudes are generally about the same as the initial altitudes.

By comparing the results presented in figure 9 with those in figure 6, it can be seen that the mission durations that can be attained are considerably higher when thrust rever-

sal is utilized than for the cases having no thrust reversal. On the other hand, the maximum altitudes attained with thrust reversal are considerably less than the final altitudes attained with no thrust reversal. For example, at an initial thrust-weight ratio of 5.0×10^{-6} and an initial altitude of 500 nautical miles (926 km), thrust reversal would yield a mission duration of 602 days compared with 433 days with no thrust reversal (solid curves). The maximum altitude attained would be 2200 nautical miles (4074.4 km) compared with 3150 nautical miles (5833.8 km) with no thrust reversal.

Also, by comparing the results presented in figures 9 and 6, it can be seen that the effects of thrust reversal on mission starting date and initial inclination are small. For example, at an initial thrust-weight ratio of 5.0×10^{-6} and an initial altitude of 500 nautical miles (926 km), the required mission starting date with thrust reversal would be August 31 compared with September 7 with no thrust reversal (solid curves). The required initial inclination would be 107.2° compared with 107.5° . It may be noted from figure 9 that the time of thrust reversal occurs at about 50 to 55 percent of the total mission duration.

A typical variation of mission duration with mission starting date is shown in figure 10 for an initial altitude of 500 nautical miles (926 km) and a thrust-weight ratio of 5.0×10^{-6} . Here again, each point on these curves is fully optimized, that is, each has an optimum initial inclination, time of thrust reversal, and ψ_0 .

Thrust Angle History

Two typical optimized time histories of η and η_c are shown in figure 11 for no thrust reversal and with thrust reversal, respectively. These curves are presented for an initial altitude of 500 nautical miles (926 km), a thrust-weight ratio of 5.0×10^{-6} and $N = +1$. The angle η_c is a function only of altitude (as described by eq. (2)) and represents the radius of the circle of tolerance. The angle η is the angle between the orbit perpendicular and the sunline and is given by equation (3). The angle η may also be thought of as the maximum angle in yaw between the thrust vector and the orbit plane during any orbit. The angle between the thrust vector and the orbit plane varies sinusoidally over one orbit with the maximum value (equal to η) occurring at the two intersection points of the orbit track and the plane perpendicular to the sunline. These intersection points are illustrated in figure 2 as points 1 and 3. Without thrust reversal (fig. 11(a)), the orbit perpendicular just approaches the edge of the circle of tolerance at about 225 days and finally leaves the circle of tolerance at about 433 days. With thrust reversal (fig. 11(b)), the orbit perpendicular just approaches the edge of the circle of tolerance at about 105 days as the altitude is increasing and again at about 510 days as the altitude is decreasing and finally leaves the circle of tolerance at about 602 days.

Validity of Approximations

The N-Body trajectory code described in reference 5 was used to investigate the relative effects of thrust, perturbations due to the Sun and the Moon, and the oblateness of the Earth on the orbit inclination, node, and eccentricity by integrating a typical mission. The secular change of either orbit inclination or nodes due to thrust was an order of magnitude greater than that due to the Sun and Moon combined. No secular change in orbit eccentricity due to either thrust or the Sun and Moon was observed. The effects of the Sun and Moon were therefore considered negligible and were validly neglected in the approximate solution of appendix B.

The secular rate of change of the orbit node due to oblateness was approximated by considering only the terms through the second harmonic in the potential function (eq. (1)). With this approximation, the secular change of nodes due to oblateness was more than two orders of magnitude greater than that due to thrust while the secular change in inclination and eccentricity was zero. The change of nodes due to higher order oblateness terms (third and fourth harmonics) was determined to be only about 0.1 percent of that due to the total oblateness force. The secular change of either inclination or eccentricity due to higher order oblateness terms is very negligible. An insignificant error results, therefore, by neglecting higher order oblateness terms in the approximate solution.

In order to study further the validity of the approximate solution of appendix B, the N-Body code was used to integrate numerically a complete mission and results compared with those of the approximate solution. The mission chosen was the overall optimum mission with no thrust reversal for an initial altitude of 500 nautical miles (926 km) and an initial thrust-weight ratio of 5.0×10^{-6} . The mission starting date was September 6 and the initial inclination was 107.61° . Orbit inclination and altitude and the angle by which the orbit perpendicular lags the Sun in longitude are shown as functions of the number of orbits traversed in figures 12(a), (b), and (c), respectively. It can be seen that the changes in these variables, as computed from the approximate solution, are very close to the numerically integrated solution obtained with the N-Body code.

The approximate solution yielded a maximum time in continuous sunlight of 433 days and the thrust angle history for this optimum case is shown in figure 11(a). The N-Body solution entered shadow at 440 days but also encountered some shadow earlier in the mission as illustrated by the thrust angle history shown in figure 11(c). The reason is that the N-Body case started with an inclination which was optimum only for the approximate solution. For the N-Body case to remain in continuous sunlight, it would be necessary to start with an inclination slightly less than that found to be optimum from the approximate solution. It is estimated that this required small change in inclination would be about 0.1° and would yield a maximum time in continuous sunlight very nearly equal to the 433 days found with the approximate method.

The computer time required for the approximate solution during which 10 complete trajectories were flown while iterating on the optimum initial inclination was about 0.5 minute. The time required for the N-Body to fly just one trajectory was about 3 hours.

Error Tolerances

The data presented in this report assume that the initial orbit conditions such as the initial inclination, altitude, and launch time of day which determines ψ_0 are exact. Furthermore, it is assumed that the electric rockets on the spacecraft produce full thrust at the start of the mission and continue to do so throughout the mission. The values of mission duration and altitude attained, then, are essentially absolute maxima.

Realistic satellite launchings will always result in some small deviation from the desired altitude, inclination, and eccentricity. Also, a reasonable launch window is desired so that a range of ψ_0 (function of launch time of day) must be accounted for as well as errors in establishing the desired ψ_0 . If these deviations in the initial orbit parameters are not accounted for, the satellite may begin the mission in shadow or may enter shadow much sooner than expected. Dispersions in the initial orbit parameters may be accounted for by biasing the initial inclination with only a small penalty in mission duration.

Biasing the initial inclination was briefly investigated for a typical mission with thrust reversal. Typical launch injection errors of ± 15 nautical miles (± 2.778 km) in orbit altitude and $\pm 0.5^\circ$ in orbit inclination were assumed. Errors in orbit eccentricity were not considered but would also have to be accounted for in any real launch.

The effects of biasing the initial inclination may be illustrated from figure 13 which shows mission duration as a function of ψ_0 for lines of constant initial inclination. These results are presented for an initial altitude of 485 nautical miles (altitude error of -15 n mi (-2.778 km)). This starting condition is more critical than an altitude error of $+15$ nautical miles ($+2.778$ km), because it results in a smaller η_c (eq. (2)) and, hence, a smaller circle of tolerance at the beginning of the mission. The data of figure 13 all have optimum thrust reversal times.

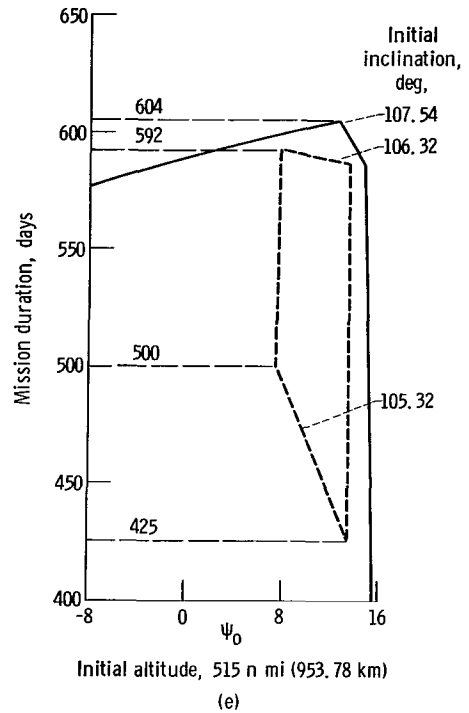
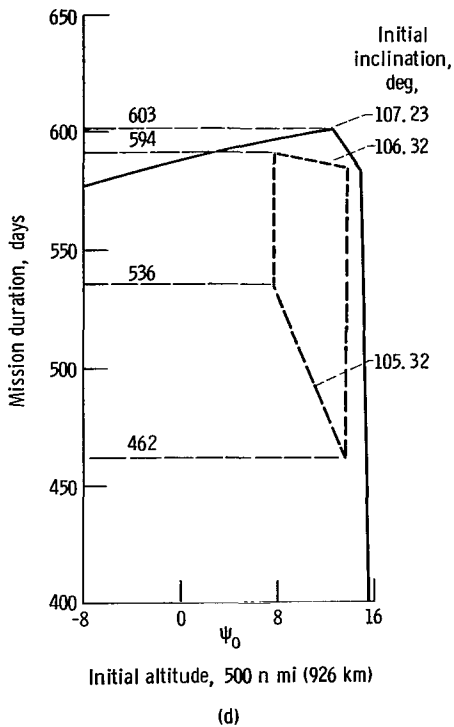
From the initial conditions presented in figure 13, there is only one initial inclination and ψ_0 which yield the maximum mission duration of 602 days. The required inclination at this point is 106.91° and the required ψ_0 is 12.52° . This case takes full advantage of the circle of tolerance by starting on the edge of the circle and again just touching the edge of the circle at the first close approach as illustrated by positions 1 and 2, respectively, in figure 5. Any other combination of initial inclination and ψ_0 within the limit lines shown in figure 13 would result in a mission duration (in sunlight) less than the maximum of 602 days. For any mission starting date, two conditions limit the possible combinations of initial inclination and ψ_0 ; (1) the necessity for starting the mission in sunlight

and (2) the requirement to remain in continuous sunlight as long as possible. The limit line to the right of figure 13 defines those missions which just start in sunlight on the edge of the circle of tolerance but do not touch the circle of tolerance at the first close approach. The limit line to the upper left of figure 13 defines those missions which start inside the circle of tolerance but just touch the circle of tolerance at the first close approach. The intersection of these two lines defines the case having the maximum mission duration. This case would just start in sunlight on the edge of the circle of tolerance and would also again just touch the circle of tolerance at the first close approach.

In order to bias the initial inclination properly to account for orbit injection errors, it is necessary to choose an inclination such that no expected dispersion in inclination from the biased nominal will exceed the limit lines of figure 13 and yet allow a reasonable launch window. Orbit altitude errors can be accounted for by choosing the lowest altitude expected, which is most critical, and then biasing the inclination at that altitude. This was done for figure 13 which is presented for an altitude of 485 nautical miles (898.22 km), corresponding to the assumed altitude error of -15 nautical miles (-2.778 km). The dashed lines shown in figure 13 define the boundaries of initial inclination and ψ_0 resulting from assuming a launch window of approximately 25 minutes and an inclination error of $\pm 0.5^\circ$. Nominally, the launch window would open at point A ($\psi_0 = 13.7^\circ$) and close at point B ($\psi_0 = 7.5^\circ$). The difference in ψ_0 of 6.2° is equivalent to 24.8 minutes of launch window since the Earth revolves 0.25° per minute. The biased nominal initial inclination is 105.82° along a line from point A to point B. For this initial inclination, the time in continuous sunlight would range from 583 days at point A to 590 days at point B. As can be seen, the nominal inclination was biased to 105.82° so that for an inclination error of $+0.5^\circ$ resulting in an initial inclination of 106.32° , the starting conditions would not exceed the limit lines of figure 13. The critical points are indicated by point C (591 days) at the opening of the launch window and point D (598 days) at the closing of the window. An inclination error of -0.5° (initial inclination of 105.32°) is not critical from the standpoint of exceeding the limit lines but will result in considerably less mission duration as indicated by points E (498 days) and F (572 days).

A launch injection error which has not been discussed as yet but which can affect the length of the launch window is the error in establishing the orbit node at precisely the proper inertial longitude. This error directly affects ψ_0 but could be accounted for by simply moving inside the boundaries on ψ_0 (13.7° and 7.5°) shown in figure 13, thereby reducing the launch window.

Although the results of figure 13 are presented for an initial altitude of 485 nautical miles (898.22 km) (corresponding to an altitude error of -15 n mi (-2.778 km) from a nominal of 500 n mi (926 km)), the initial altitude may range from 485 to 515 nautical miles (898.22 to 953.78 km) (± 15 n mi (± 2.778 km)) depending on the accuracy of the launch. For altitudes greater than 485 nautical miles (898.22 km), the results would be



similar to those shown in figure 13 except that the scale on initial inclination would be shifted progressively higher for higher altitudes. In other words, the dashed boundary of figure 13 would shift progressively lower in the figure with respect to the limit lines. This is illustrated in sketches (d) and (e) for initial altitudes of 500 and 515 nautical miles (926.00 and 953.78 km), respectively. As seen in sketches (d) and (e), the overall optimum point at 500 nautical miles (926.78 km) would have an initial inclination of 107.23° and at 515 nautical miles (953.78 km) an inclination of 107.54° compared with 106.91° at 485 nautical miles (898.22 km). The maximum mission duration for these three altitudes is nearly a constant. At the same time, the initial inclination limits for the launch would always range from 105.32° to 106.32° (lower and upper lines of dashed boundary) determined from biasing the initial inclination to 105.82° at 485 nautical miles (898.22 km) (fig. 13). The dashed boundary, therefore, will shift progressively lower with respect to the overall optimum point as indicated in sketches (d) and (e).

It can be seen then, that if the initial altitude were 500 nautical miles (926 km) (sketch (d)), the mission durations would range from about 594 days at point D down to about 462 days at point E. If the initial altitude were 515 nautical miles (953.78 km) (sketch (e)), the mission durations would range from about 592 days at point D down to about 425 days at point E. These may be compared with 598 days at point D and 498 days at point E for starting at an initial altitude of 485 nautical miles (898.22 km).

CONCLUDING REMARKS

It has been shown that a low-thrust, Earth satellite mission planned around the concept of remaining in continuous sunlight and utilizing tangential thrusting in a plane perpendicular to the sunline may be analyzed by using the approximate numerical method presented in this report. This thrust-vector orientation would allow use of a spacecraft with fixed solar panels and thrusters, and attitude control could be implemented by using horizon scanners and Sun seekers. Although the analysis and results presented in this report were obtained for a satellite having a particular thrust vector orientation with respect to the orbit plane and the Sun, the approach to the problem and method of solution would be generally applicable to other low-thrust, circular Earth orbit missions having out-of-plane thrusting. The results obtained by using this approximate method exhibit a high degree of accuracy when compared with numerically integrated solutions.

The time that an Earth satellite remains in continuous sunlight can be maximized by a choice of proper initial orbit parameters. These initial conditions were determined for a range of thrust-weight ratios and initial altitudes for thrusting tangentially in a plane perpendicular to the sunline. For comparison purposes, tangential thrusting in the orbit plane was also investigated. For the low thrust-weight ratios studied, the thrust component normal to the orbit plane had little effect on the mission duration. The greatest effect of the normal component of thrust was to reduce the maximum altitude achieved.

The effect of reversing the thrust during the latter part of the mission was also investigated. Optimum thrust reversal times occurred at 50 to 55 percent of the total mission duration. It was shown that thrust reversal can significantly increase the time spent in continuous sunlight.

All the orbits studied have inclinations greater than 90° so that all orbits are retrograde. Optimum initial inclinations increase with increasing thrust-weight ratio and increasing initial altitude. The combination of initial altitude, weight of the satellite and the initial inclination required is important in determining the orbital payload capability required of the launch vehicle.

Mission duration increases with increasing initial altitude and decreasing initial thrust-weight ratio. The maximum altitude achieved, on the other hand, increases with both increasing initial altitude and initial thrust-weight ratio.

Errors in establishing the initial orbit conditions, as well as starting the mission at a time other than the optimum, can cause some of the orbits during the mission to encounter shadow. It was shown that shadowing may be eliminated by biasing the initial in-

clination to account for these deviations. This would reduce the time spent in continuous sunlight below the maximum mission durations presented in this report.

Lewis Research Center,
National Aeronautics and Space Administration,
Cleveland, Ohio, March 17, 1967,
124-06-01-02-22.

APPENDIX A

SYMBOLS

A	total thrust acceleration, ft/sec^2 (m/sec^2)
B	constant (see appendix B)
C	circumferential thrust acceleration, ft/sec^2 (m/sec^2)
D	constant (see appendix C)
E	constant (see appendix C)
g	acceleration of gravity on equator at surface of Earth, $32.174 \text{ ft}/\text{sec}^2$ ($9.8066352 \text{ m}/\text{sec}^2$)
h	altitude of satellite above equatorial radius, ft (m)
I	orbit inclination, deg
J	coefficient of second harmonic in gravitational potential function, 1.62345×10^{-3}
K_1, K_2, K_3, K_4	constants (see appendix B)
K^*, K^{**}	constants (see appendix B)
N	orbit index equal to +1 if sunline is on same side of orbit plane as orbit perpendicular or equal to -1 if sunline is on opposite side
R_E	Earth equatorial radius, 20925738.0 ft (6378.165 km)
r	radius of satellite from center of Earth, ft(m)
t	time, sec
u	instantaneous angular position of satellite in orbit plane measured from ascending node positively in direction of motion, deg
W	thrust acceleration normal to orbit plane measured positively in the di- rection of the orbital angular velocity vector, ft/sec^2 (m/sec^2)
X, Y, Z	Earth centered inertial rectangular coordinates with X pointing in direc- tion of vernal equinox and with X and Y lying in equatorial plane and Z in right-hand relation
X', Y', Z'	Earth centered instantaneous rectangular coordinates referenced to po- sition of Sun with Z' pointing in direction of Sun and X' perpendicu- lar to Z' and lying in equatorial plane and Y' in right-hand relation; primes denote coordinate system used when Sun is in on side of orbit plane opposite to orbit perpendicular

X'', Y'', Z''	similar to X', Y', Z' except used for case where Sun is on same side of orbit plane as orbit perpendicular
α	right ascension of Sun measured positively counterclockwise from vernal equinox to projection of sunline in equatorial plane, deg
γ	angle by which θ leads (or lags) u , θ -Nu, deg
δ	declination of Sun measured positively above equator, negative below, deg
η	angle between orbit plane and plane perpendicular to sunline or between orbital angular velocity vector (or its negative whichever yields smaller angle), and sunline, deg
η_c	maximum η allowable for orbit to remain in continuous sunlight, deg
θ	angular position in plane perpendicular to sunline (corresponds to u in orbit plane) measured positively from X' toward Y' counterclockwise about Z' (sunline opposite to orbit perpendicular) or measured positively from X'' toward Y'' counterclockwise about Z'' (sunline on same side as orbit perpendicular); angle θ is obtained by projecting satellite position in the orbit into plane perpendicular to sunline along great circle which forms spherical isosceles triangle with orbit plane and plane perpendicular to sunline, deg
μ	gravitational constant of Earth, $1.4076539 \times 10^{16} \text{ ft}^3/\text{sec}^2$ ($3.9860319 \times 10^{14} \text{ m}^3/\text{sec}^2$)
ψ	angle by which orbit perpendicular lags Sun in longitude, $\alpha - \Omega$, deg
ω	angular velocity of satellite, rad/sec
Ω	right ascension of orbit perpendicular, measured positively counterclockwise from vernal equinox to projection of orbit perpendicular in equatorial plane, deg

Subscripts:

av	average
max	maximum
min	minimum
0	initial conditions
1	intermediate values for matrix

Superscript:

*	indicates constant angle for one orbit (see appendix C)
---	---

Since the thrust vector is constrained to be always tangential and in a plane perpendicular to the sunline, the acceleration components perpendicular to the sunline and along the sunline are

$$\left. \begin{aligned} A_{X'} &= A_{X''} = -NA \sin \theta \\ A_{Y'} &= A_{Y''} = NA \cos \theta \\ A_{Z'} &= A_{Z''} = 0 \end{aligned} \right\} \quad (B1)$$

where θ is measured differently between the X' and X'' systems (see appendix A).

These acceleration components can now be expressed in the X, Y, Z system by rotating the X', Y', Z' system into the X, Y, Z system.

For the case where the sunline is on the side opposite to the orbit perpendicular, the X', Y', Z' system may be rotated counterclockwise about X' by an amount equal to $(90^\circ - \delta)$.

$$\begin{bmatrix} X'_1 \\ Y'_1 \\ Z'_1 \end{bmatrix} = \begin{bmatrix} 1 & 0 & 0 \\ 0 & \sin \delta & \cos \delta \\ 0 & -\cos \delta & \sin \delta \end{bmatrix} \begin{bmatrix} X' \\ Y' \\ Z' \end{bmatrix} \quad (B2)$$

For the case where the sunline is on the same side as the orbit perpendicular, the X'', Y'', Z'' system can be rotated counterclockwise about X'' by an amount equal to $[90^\circ + (-\delta)] = (90^\circ - \delta)$. This rotation ($N = +1$) is identical to the preceding case ($N = -1$), and equation (B2) then describes the first rotation for both $N = +1$ and $N = -1$.

The second rotation is needed now to aline the X'_1, Y'_1, Z'_1 system with the X, Y, Z system.

For the ($N = -1$) case, the X'_1, Y'_1, Z'_1 system can be rotated clockwise about Z'_1 by an amount equal to $-(\alpha - 90^\circ) = (90^\circ - \alpha)$ or, for the ($N = +1$) case, the X''_1, Y''_1, Z''_1 systems can be rotated clockwise about Z''_1 by an amount equal to $-(\alpha - 270^\circ) = (270^\circ - \alpha)$.

Here again, the rotation for either case is equivalent and can be written as

$$\begin{bmatrix} X \\ Y \\ Z \end{bmatrix} = \begin{bmatrix} \sin \alpha & \cos \alpha & 0 \\ -\cos \alpha & \sin \alpha & 0 \\ 0 & 0 & 1 \end{bmatrix} \begin{bmatrix} X'_1 \\ Y'_1 \\ Z'_1 \end{bmatrix} \quad (B3)$$

Now, combining the two rotations by matrix multiplication yields

$$\begin{bmatrix} X \\ Y \\ Z \end{bmatrix} = \begin{bmatrix} \sin \alpha & \cos \alpha & 0 \\ -\cos \alpha & \sin \alpha & 0 \\ 0 & 0 & 1 \end{bmatrix} \begin{bmatrix} 1 & 0 & 0 \\ 0 & \sin \delta & \cos \delta \\ 0 & -\cos \delta & \sin \delta \end{bmatrix} \begin{bmatrix} X' \\ Y' \\ Z' \end{bmatrix}$$

$$\begin{bmatrix} X \\ Y \\ Z \end{bmatrix} = \begin{bmatrix} \sin \alpha & \cos \alpha \sin \delta & \cos \alpha \cos \delta \\ -\cos \alpha & \sin \alpha \sin \delta & \sin \alpha \cos \delta \\ 0 & -\cos \delta & \sin \delta \end{bmatrix} \begin{bmatrix} X' \\ Y' \\ Z' \end{bmatrix} \quad (B4)$$

As is explained later, the rotation matrix of equation (B4) can be considered constant. Therefore, twice differentiating equations (B4) yields

$$A_X = A_{X'} \sin \alpha + A_{Y'} \cos \alpha \sin \delta + A_{Z'} \cos \alpha \cos \delta$$

$$A_Y = -A_{X'} \cos \alpha + A_{Y'} \sin \alpha \sin \delta + A_{Z'} \sin \alpha \cos \delta$$

$$A_Z = 0 - A_{Y'} \cos \delta + A_{Z'} \sin \delta$$

Now, substituting from equations (B1) yields

$$\left. \begin{aligned} A_X &= -NA \sin \theta \sin \alpha + NA \cos \theta \cos \alpha \sin \delta \\ A_Y &= NA \sin \theta \cos \alpha + NA \cos \theta \sin \alpha \sin \delta \\ A_Z &= -NA \cos \theta \cos \delta \end{aligned} \right\} \quad (B5)$$

Since θ is an unknown angle for this problem, it is now necessary to define θ in terms of other known angles. From spherical trigonometry (see appendix C):

$$\left. \begin{aligned} \sin \theta &= DN \sin u + E \cos u \\ \cos \theta &= D \cos u - EN \sin u \end{aligned} \right\} \quad (B6)$$

Therefore, by substituting equations (B6) into equations (B5)

$$A_X = -NA \left[(DN \sin u + E \cos u) \sin \alpha - (D \cos u - EN \sin u) \cos \alpha \sin \delta \right]$$

$$A_Y = NA \left[(DN \sin u + E \cos u) \cos \alpha + (D \cos u - EN \sin u) \sin \alpha \sin \delta \right]$$

$$A_Z = -NA \left[(D \cos u - EN \sin u) \cos \delta \right]$$

or

$$\left. \begin{aligned} A_X &= -NA \left[(DN \sin \alpha + EN \cos \alpha \sin \delta) \sin u - (D \cos \alpha \sin \delta - E \sin \alpha) \cos u \right] \\ A_Y &= NA \left[(DN \cos \alpha - EN \sin \alpha \sin \delta) \sin u + (D \sin \alpha \sin \delta + E \cos \alpha) \cos u \right] \\ A_Z &= -NA \left[-EN \cos \delta \sin u + D \cos \delta \cos u \right] \end{aligned} \right\} \quad (B7)$$

Now, from reference 6, the perturbative acceleration due to the thrust component normal to the orbit plane is

$$W = A_X \cos \Delta \sin I + A_Y \sin \Delta \sin I + A_Z \cos I \quad (B8)$$

and is measured positively in the direction of the angular velocity vector. Note that the angle Δ as used in this development is 270° greater than the angle Δ from reference 6. Substituting equations (B7) into equation (B8) yields:

$$\begin{aligned} W = NA \left\{ \right. & \left[-(DN \sin \alpha + EN \cos \alpha \sin \delta) \sin u + (D \cos \alpha \sin \delta - E \sin \alpha) \cos u \right] \cos \Delta \sin I \\ & + \left[(DN \cos \alpha - EN \sin \alpha \sin \delta) \sin u + (D \sin \alpha \sin \delta \right. \\ & \left. + E \cos \alpha) \cos u \right] \sin \Delta \sin I - \left. \left[-EN \cos \delta \sin u + D \cos \delta \cos u \right] \cos I \right\} \end{aligned}$$

Now multiplying and combining terms yields

$$\begin{aligned} W = NA \left[\right. & DN \cos \alpha \sin \Delta \sin I \sin u - DN \sin \alpha \cos \Delta \sin I \sin u \\ & - EN \sin \alpha \sin \delta \sin \Delta \sin I \sin u - EN \cos \alpha \sin \delta \cos \Delta \sin I \sin u \\ & + EN \cos \delta \cos I \sin u + D \cos \alpha \sin \delta \cos \Delta \sin I \cos u \\ & + D \sin \alpha \sin \delta \sin \Delta \sin I \cos u - E \sin \alpha \cos \Delta \sin I \cos u \\ & \left. + E \cos \alpha \sin \Delta \sin I \cos u - D \cos \delta \cos I \cos u \right] \end{aligned}$$

or

$$\begin{aligned}
W = NA & \left[DN \sin I \sin u (\cos \alpha \sin \Delta\Omega - \sin \alpha \cos \Delta\Omega) - EN \sin \delta \sin I \sin u (\sin \alpha \sin \Delta\Omega \right. \\
& + \cos \alpha \cos \Delta\Omega) + EN \cos \delta \cos I \sin u - D \cos \delta \cos I \cos u \\
& + D \sin \delta \sin I \cos u (\cos \alpha \cos \Delta\Omega + \sin \alpha \sin \Delta\Omega) \\
& \left. - E \sin I \cos u (\sin \alpha \cos \Delta\Omega - \cos \alpha \sin \Delta\Omega) \right]
\end{aligned}$$

Now,

$$\psi = \alpha - \Delta\Omega$$

Therefore

$$\begin{aligned}
W = NA & \left[(-DN \sin I \sin \psi - EN \sin \delta \sin I \cos \psi + EN \cos \delta \cos I) \sin u \right. \\
& \left. + (D \sin \delta \sin I \cos \psi - E \sin I \sin \psi - D \cos \delta \cos I) \cos u \right]
\end{aligned}$$

Also, from reference 6, for a circular orbit

$$\dot{I} = \left(\sqrt{\frac{r}{\mu}} \cos u \right) W \quad (B9)$$

$$\dot{\Delta\Omega} = \left(\sqrt{\frac{r}{\mu}} \frac{\sin u}{\sin I} \right) W \quad \text{for } I \neq 0 \quad (B10)$$

In order to arrive at a closed form solution for \dot{I} and $\dot{\Delta\Omega}$, it is necessary to assume that over the period of one orbit, none of the orbit parameters change, except u , of course; that is, for one orbit, I , $\Delta\Omega$, α , δ , ψ , and r are constant with u being the independent variable of integration; therefore, let

$$B = \sqrt{\frac{r}{\mu}}$$

$$K_1 = D \quad (\text{see appendix C for } D \text{ and } E)$$

$$K_2 = E$$

$$K_3 = \sin I \sin \psi$$

$$K_4 = \sin \delta \sin I \cos \psi - \cos \delta \cos I$$

Then, W can be written as

$$W = -A \left[(K_2 K_4 + K_1 K_3) \sin u + N(K_2 K_3 - K_1 K_4) \cos u \right] \quad (B11)$$

Substituting equation (B11) into equations (B9) and (B10), yields

$$\dot{I} = -AB \left[(K_2 K_4 + K_1 K_3) \sin u \cos u - N(K_1 K_4 - K_2 K_3) \cos^2 u \right]$$

$$\dot{\Delta\Omega} = \frac{-AB}{\sin I} \left[(K_2 K_4 + K_1 K_3) \sin^2 u - N(K_1 K_4 - K_2 K_3) \sin u \cos u \right]$$

Now, let

$$K^* = -AB(K_2 K_4 + K_1 K_3)$$

$$K^{**} = NAB(K_1 K_4 - K_2 K_3)$$

Then,

$$\dot{I} = K^* \sin u \cos u + K^{**} \cos^2 u$$

$$\dot{\Delta\Omega} = \frac{1}{\sin I} (K^* \sin^2 u + K^{**} \sin u \cos u)$$

Since u is the independent variable, integration must be made with respect to u . Let

$$du = \omega dt$$

where ω is the angular velocity of the vehicle and is assumed to be constant over one orbit. Therefore,

$$dI = \frac{1}{\omega} (K^* \sin u \cos u + K^{**} \cos^2 u) du$$

$$d\Delta\Omega = \frac{1}{\omega \sin I} (K^* \sin^2 u + K^{**} \sin u \cos u) du$$

Integrating yields

$$I = \frac{1}{\omega} \left[K^* \left(\frac{1}{2} \sin^2 u \right) + K^{**} \left(\frac{1}{2} u + \frac{1}{4} \sin 2u \right) \right] + I_0$$

$$\Delta \Omega = \frac{1}{\omega \sin I} \left[K^* \left(\frac{1}{2} u - \frac{1}{4} \sin 2u \right) + K^{**} \left(\frac{1}{2} \sin^2 u \right) \right] + \Delta \Omega_0$$

The periodic terms over one orbit, can be neglected and the secular changes in I and $\Delta \Omega$ due to W are just

$$\left. \begin{aligned} \Delta I &= \frac{1}{2\omega} K^{**} \Delta u \\ \Delta \Omega &= \frac{1}{2\omega \sin I} K^* \Delta u \end{aligned} \right\} \quad (\text{B12})$$

From reference 2, the change of altitude as a function of time for a circular orbit is given by

$$\frac{dh}{dt} = \frac{2\sqrt{g}}{R_E} \frac{C}{g} (R_E + h)^{3/2}$$

Now, since

$$du = \omega dt = \frac{\sqrt{\mu}}{(R_E + h)^{3/2}} dt$$

then

$$dh = \frac{2C}{\sqrt{\mu} R_E \sqrt{g}} (R_E + h)^3 du \quad (\text{B13})$$

The circumferential thrust acceleration C is a function of u and varies periodically over one orbit. Therefore, over one orbit, C can be taken as a constant, that is,

$$C_{av} = \frac{C_{max} + C_{min}}{2}$$

where

$$C_{\max} = A$$

and

$$C_{\min} = A \cos \eta$$

Integrating equation (B13) yields

$$(R_E + h_0)^{-2} - (R_E + h)^{-2} = \frac{4C_{av}}{\sqrt{\mu} R_E \sqrt{g}} \Delta u \quad (B14)$$

From equation (B14), the change in altitude from h_0 to h can thus be found with a change in u , Δu .

Also from reference 2, the nodal precession of the orbit due to oblateness can be expressed as

$$\dot{\Omega} \approx - \sqrt{\mu} J R_E^2 (R_E + h)^{-7/2} \cos I$$

therefore,

$$d\Omega = \frac{-\sqrt{\mu} J}{\omega R_E^{3/2}} \cos I \left(\frac{R_E}{R_E + h} \right)^{7/2} du$$

Substituting for ω and for du from equation (B13) gives

$$d\Omega = - \sqrt{\mu g} \frac{J R_E^3}{2C_{av}} \cos I (R_E + h)^{-5} dh$$

Integrating

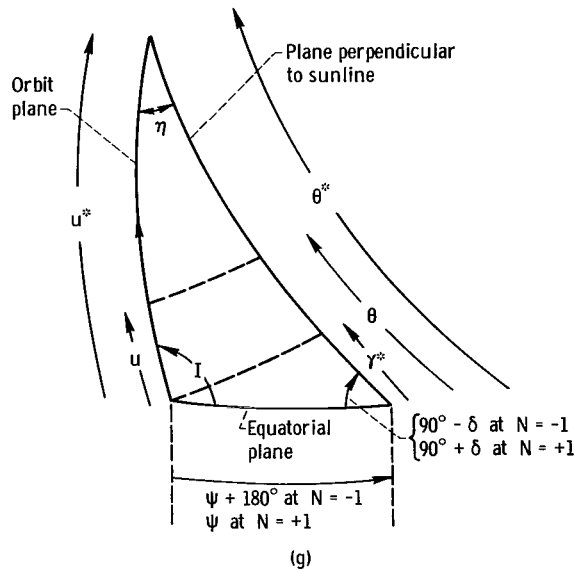
$$\Delta\Omega = - \sqrt{\mu g} \frac{J R_E^3}{8C_{av}} \cos I \left[(R_E + h_0)^{-4} - (R_E + h)^{-4} \right] \quad (B15)$$

Therefore, from equation (B15) the nodal precession due to oblateness can be found after the change in altitude has been found. This can be combined with equation (B12) to give the total change in nodes.

APPENDIX C

EQUATIONS DEFINING ANGULAR POSITION IN PLANE PERPENDICULAR TO SUNLINE IN TERMS OF KNOWN ANGLES

Consider the spherical triangle formed by the orbit plane, the plane perpendicular to the sunline and the equatorial plane in sketch (g). Let u^* , θ^* , and γ^* be angles which have a long term variation with time but may be considered constants for one or even several orbits. The angle u^* is measured positively from the ascending node ($u = 0$) to the point of intersection of the orbit plane with the plane perpendicular to the sunline; θ^* is measured negatively from the equator to the intersection of the planes; and γ^* is measured with the same sense as θ^* and is the amount that θ leads (or lags) u (see



appendix A for definitions of u and θ). When $u = 0$, $\theta = \gamma^*$. Now, from sketch (g),

$$Nu^* = \theta^* - \gamma^*$$

for

$$0^\circ \leq u^* \leq +180^\circ$$

$$-180^\circ \leq \theta^* \leq 0^\circ$$

or

$$\gamma^* = \theta^* - Nu^*$$

Also,

$$\theta = \gamma^* + Nu + 360^0 = (\theta^* - Nu^*) + (Nu + 360^0)$$

Therefore, expanding yields

$$\sin \theta = \sin(\theta^* - Nu^*)\cos(Nu + 360^0) + \cos(\theta^* - Nu^*)\sin(Nu + 360^0)$$

$$\sin \theta = (\sin \theta^* \cos Nu^* - \cos \theta^* \sin Nu^*) (\cos Nu \cos 360^0 - \sin Nu \sin 360^0)$$

$$+ (\cos \theta^* \cos Nu^* + \sin \theta^* \sin Nu^*) (\sin Nu \cos 360^0 + \cos Nu \sin 360^0)$$

Now, since

$$\cos Nu^* = \cos u^*$$

and

$$\sin Nu^* = N \sin u^*$$

$$\sin \theta = (\sin \theta^* \cos u^* - N \cos \theta^* \sin u^*)\cos u + (\cos \theta^* \cos u^* + N \sin \theta^* \sin u^*)N \sin u$$

or

$$\sin \theta = N \sin u(\cos u^* \cos \theta^* + N \sin u^* \sin \theta^*)$$

$$+ \cos u(\cos u^* \sin \theta^* - N \sin u^* \cos \theta^*) \quad (C1)$$

Similarly,

$$\cos \theta = \cos(\theta^* - Nu^*)\cos(Nu + 360^0) - \sin(\theta^* - Nu^*)\sin(Nu + 360^0)$$

$$\cos \theta = (\cos \theta^* \cos Nu^* + \sin \theta^* \sin Nu^*) (\cos Nu \cos 360^0 - \sin Nu \sin 360^0)$$

$$- (\sin \theta^* \cos Nu^* - \cos \theta^* \sin Nu^*) (\sin Nu \cos 360^0 + \cos Nu \sin 360^0)$$

Therefore,

$$\begin{aligned} \cos \theta &= \cos u(\cos u^* \cos \theta^* + N \sin u^* \sin \theta^*) \\ &\quad - N \sin u(\cos u^* \sin \theta^* - N \sin u^* \cos \theta^*) \end{aligned} \quad (C2)$$

From equations (C1) and (C2), let

$$D = \cos u^* \cos \theta^* + N \sin u^* \sin \theta^*$$

$$E = \cos u^* \sin \theta^* - N \sin u^* \cos \theta^*$$

Therefore,

$$\sin \theta = DN \sin u + E \cos u$$

$$\cos \theta = D \cos u - EN \sin u$$

Now u^* and θ^* can be found in terms of other known angles. Referring again to sketch (g) and using the law of sines and the law of cosines gives, for $N = -1$,

$$\sin u^* = \frac{\sin(90^\circ - \delta)\sin(\psi + 180^\circ)}{\sin \eta} = -\frac{\cos \delta \sin \psi}{\sin \eta}$$

$$\cos u^* = \frac{\cos(90^\circ - \delta) + \cos I \cos \eta}{\sin I \sin \eta} = \frac{\sin \delta + \cos \eta \cos I}{\sin I \sin \eta}$$

and, for $N = +1$,

$$\sin u^* = \frac{\sin(90^\circ + \delta)\sin \psi}{\sin \eta} = \frac{\cos \delta \sin \psi}{\sin \eta}$$

$$\cos u^* = \frac{\cos(90^\circ + \delta) + \cos I \cos \eta}{\sin I \sin \eta} = \frac{-\sin \delta + \cos I \cos \eta}{\sin I \sin \eta}$$

Therefore, in general,

$$\left. \begin{aligned} \sin u^* &= N \frac{\cos \delta \sin \psi}{\sin \eta} \\ \cos u^* &= \frac{-N \sin \delta + \cos \eta \cos I}{\sin \eta \sin I} \end{aligned} \right\} \quad (C3)$$

Likewise, for $N = -1$,

$$\sin \theta^* = -\frac{\sin I \sin(\psi + 180^\circ)}{\sin \eta} = \frac{\sin I \sin \psi}{\sin \eta}$$

$$\cos \theta^* = \frac{\cos I + \cos(90^\circ - \delta)\cos \eta}{\sin(90^\circ - \delta)\sin \eta} = \frac{\cos I + \sin \delta \cos \eta}{\cos \delta \sin \eta}$$

and, for $N = +1$,

$$\sin \theta^* = -\frac{\sin(180^\circ - I)\sin \psi}{\sin \eta} = -\frac{\sin I \sin \psi}{\sin \eta}$$

$$\cos \theta^* = \frac{\cos(180^\circ - I) + \cos(90^\circ - \delta)\cos \eta}{\sin(90^\circ - \delta)\sin \eta} = \frac{-\cos I + \sin \delta \cos \eta}{\cos \delta \sin \eta}$$

Therefore, in general,

$$\left. \begin{aligned} \sin \theta^* &= -\frac{N \sin I \sin \psi}{\sin \eta} \\ \cos \theta^* &= \frac{-N \cos I + \sin \delta \cos \eta}{\cos \delta \sin \eta} \end{aligned} \right\} \quad (C4)$$

It is seen that u^* and θ^* are functions only of δ , ψ , η , and I , which are assumed constant for one orbit. In order for equations (C3) and (C4) to be evaluated correctly, it is important that, for $N = +1$, $\psi = \psi$, and for $N = -1$, $\psi = \psi + 180^\circ$.

REFERENCES

1. Hanson, James N.; and Fairweather, Stephen H.: Nodal Rotation for Continuous Exposure of an Earth Satellite to the Sun. ARS J., vol. 31, no. 5, May 1961, pp. 640-645.
2. Brown, Dennis W.: Low-Thrust Orbit Raising in Continuous Sunlight. NASA TN D-2072, 1964.
3. Willis, Edward A., Jr.: Finite-Thrust Escape from and Capture into Circular and Elliptic Orbits. NASA TN D-3606, 1966.
4. Ehricke, Krafft A.: Dynamics. Vol. II of Spaceflight. D. Van Nostrand Co., Inc., 1962.
5. Strack, William C.; and Huff, Vearl N.: The N-Body Code - A General Fortran Code for the Numerical Solution of Space Mechanics Problems on an IBM 7090 Computer. NASA TN D-1730, 1963.
6. Dobson, Wilbur F.; Huff, Vearl N.; and Zimmerman, Arthur V.: Elements and Parameters of the Osculating Orbit and Their Derivatives. NASA TN D-1106, 1962.

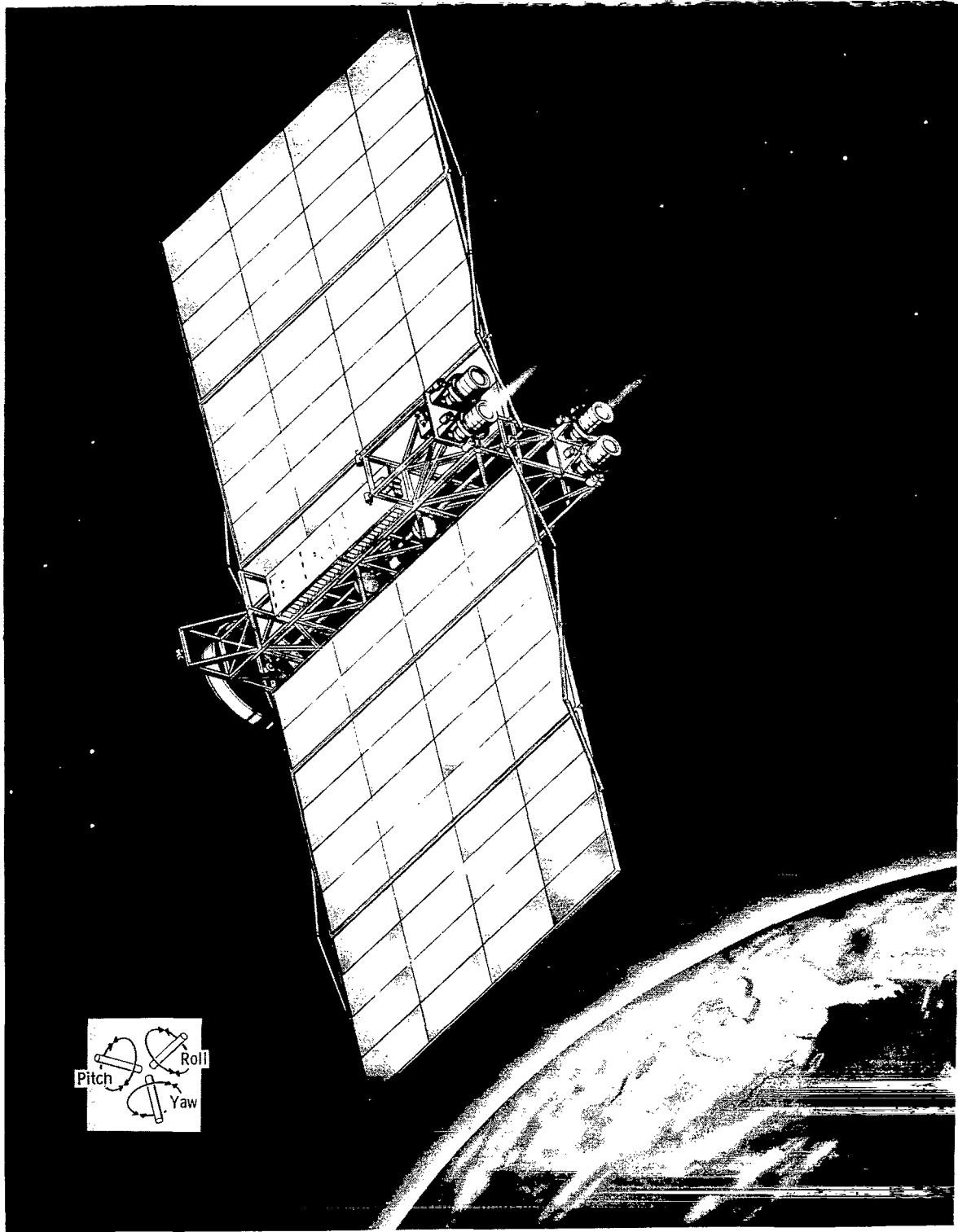


Figure 1. - Conceptual spacecraft configuration with solar cell panels.

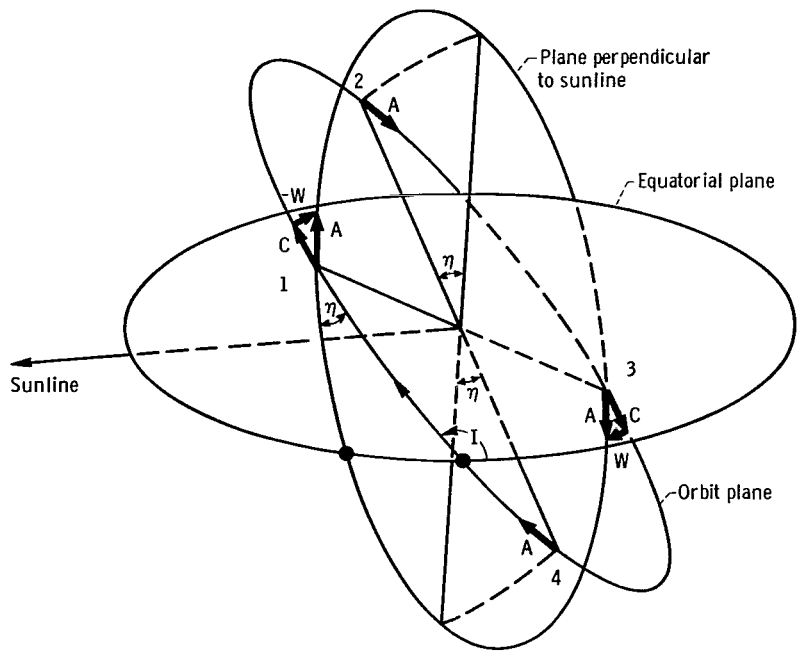


Figure 2. - Periodic variation of acceleration vector over one orbit. (Numbers denote orbital positions.)

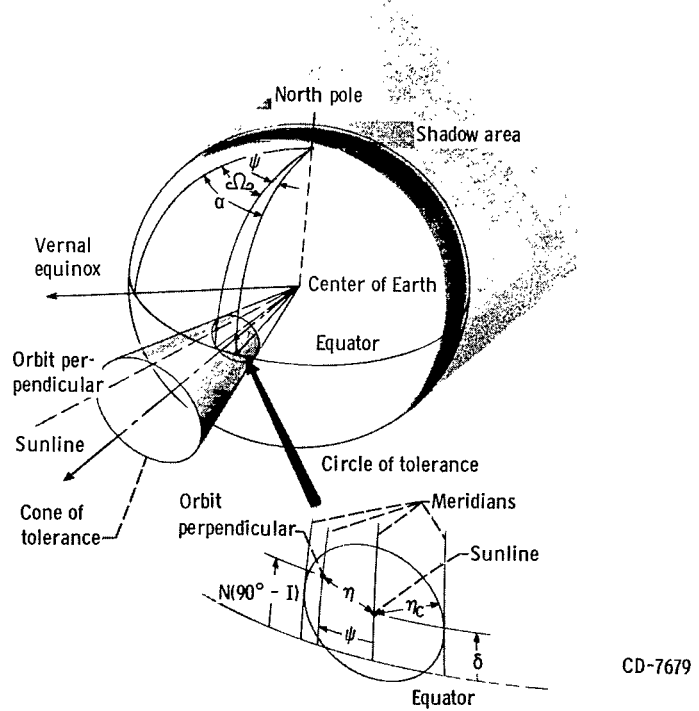


Figure 3. - Cone of tolerance associated with Earth (taken from ref. 2).

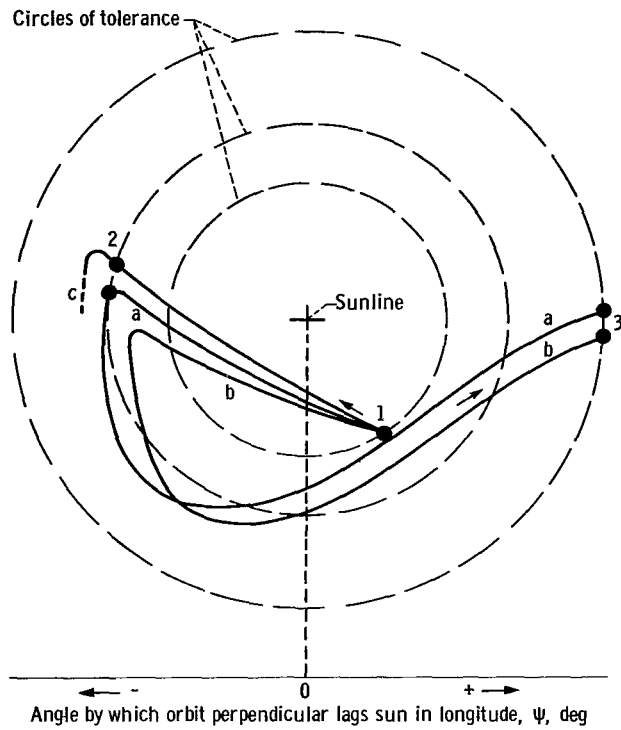


Figure 4. - Typical paths of orbit perpendicular within circle of tolerance. Orbit index, +1. (Letters denote path of orbit perpendicular; numbers denote position of orbit perpendicular.)

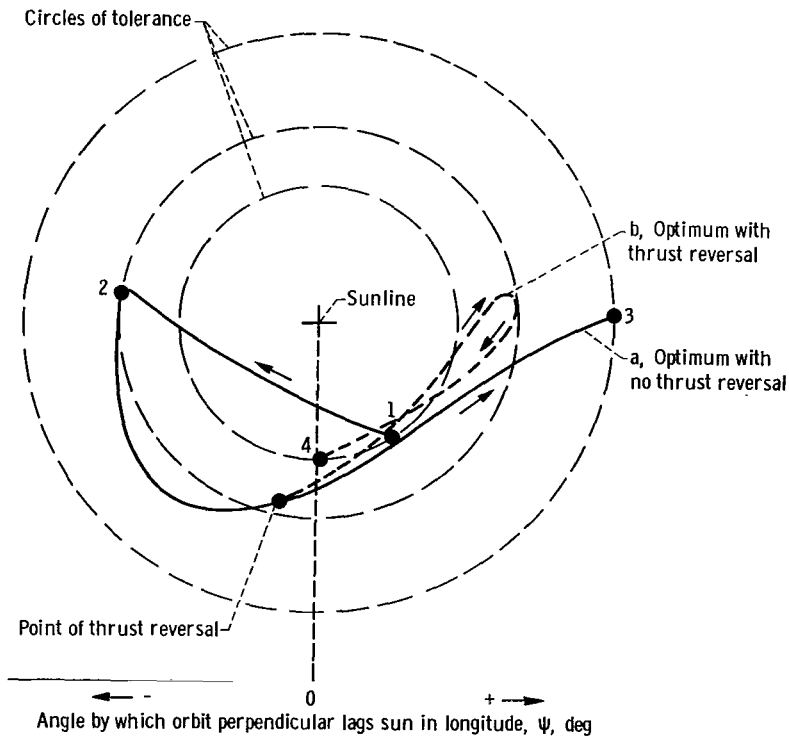


Figure 5. - Typical optimum paths of orbit perpendicular within circle of tolerance with and without thrust reversal. Orbit index, +1.

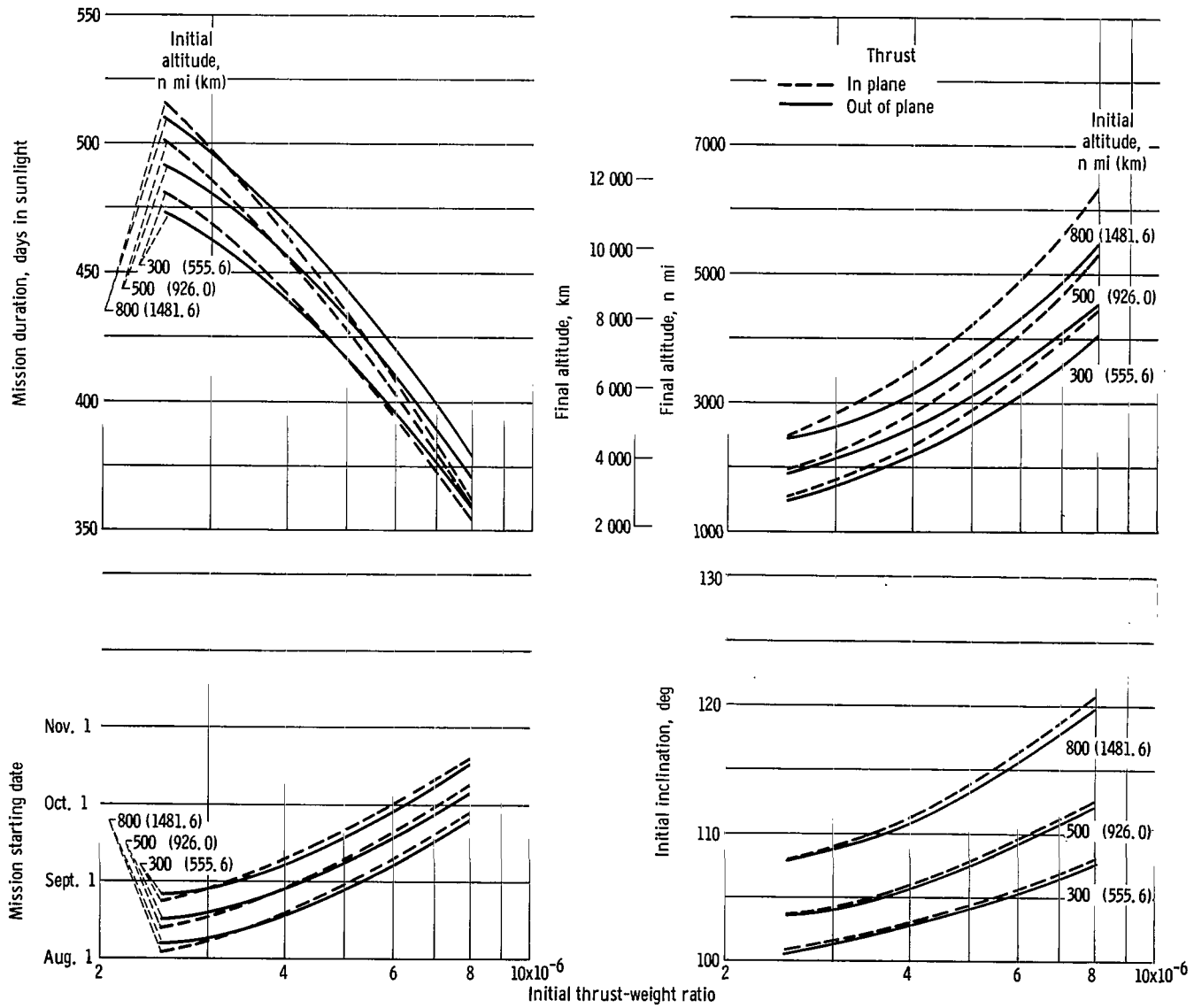


Figure 6. - Optimum mission variables as function of thrust-weight ratio. Orbit index, +1.

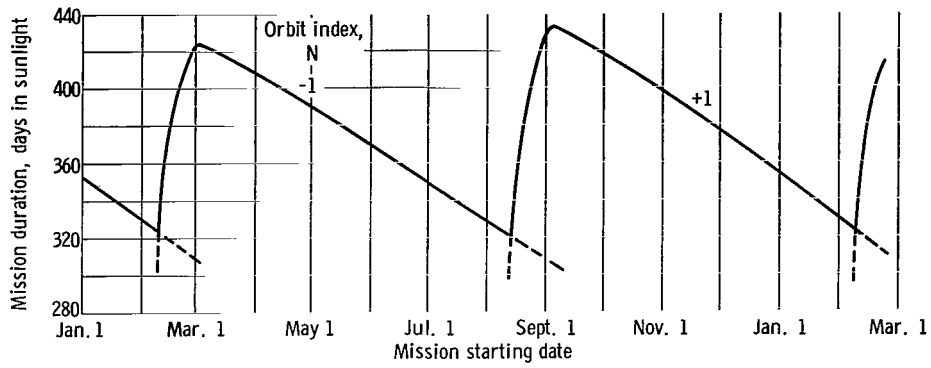


Figure 7. - Maximum mission duration as function of mission starting date. Initial altitude, 500 nautical miles; initial thrust-weight ratio, 5.0×10^{-6} ; tangential thrusting in plane perpendicular to sunline.

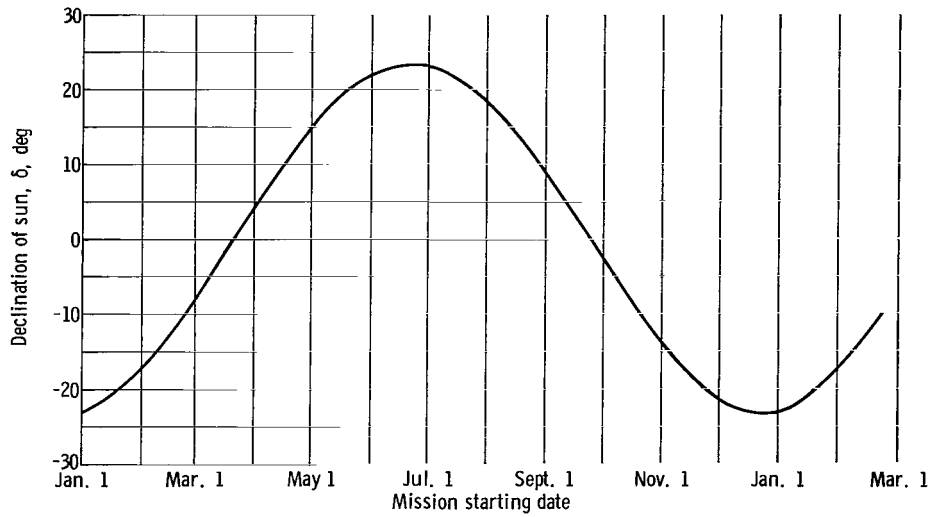


Figure 8. - Mean declination of sun as function of mission starting date.

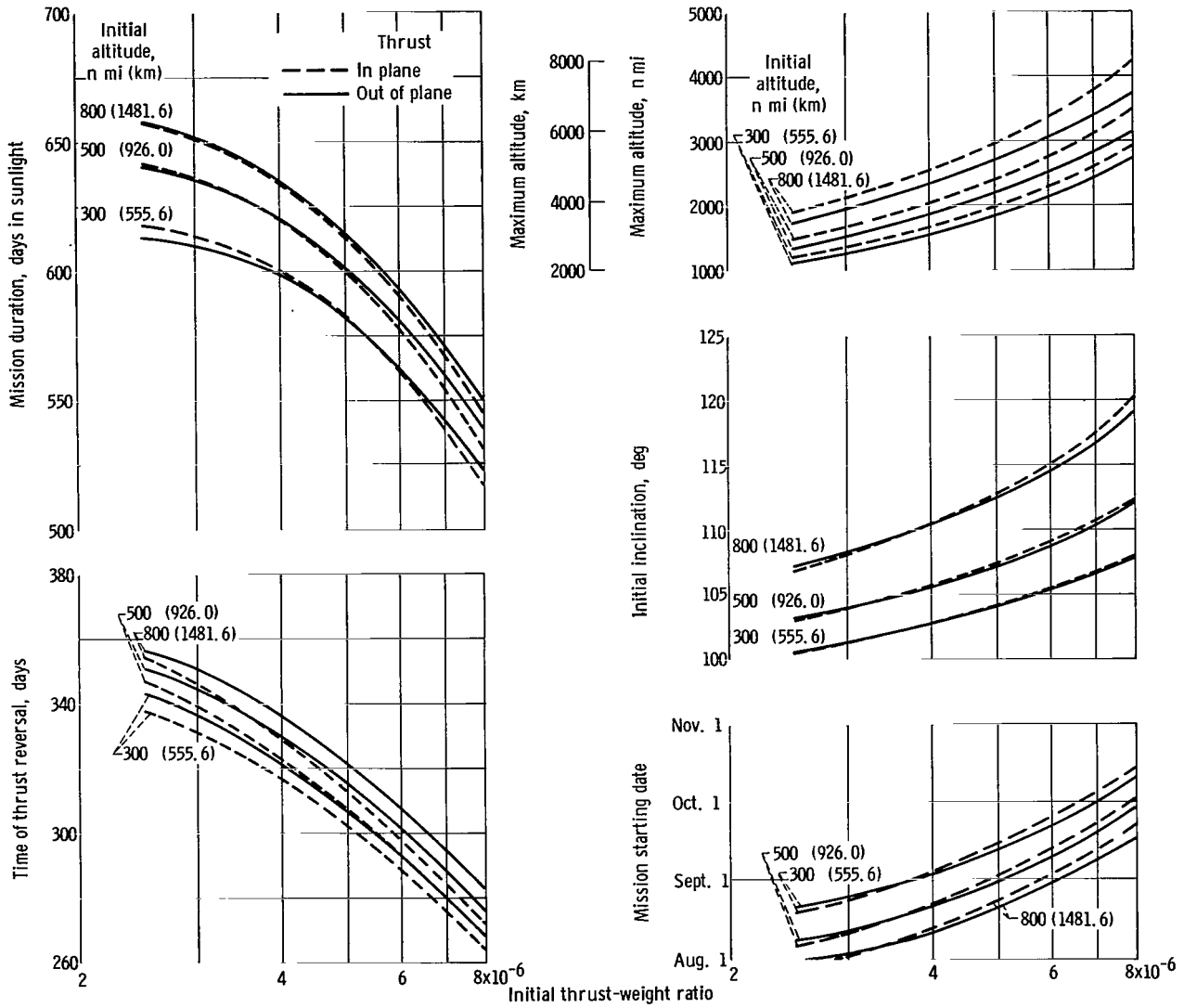


Figure 9. - Optimum mission variables as function of thrust-weight with thrust reversal used. Orbit index, +1.

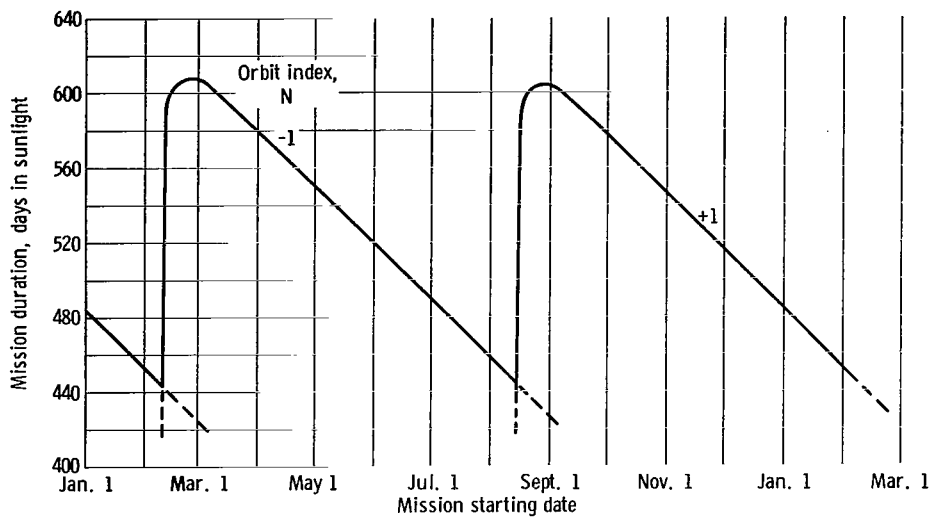


Figure 10. - Mission duration as function of mission starting date with thrust reversal. Initial altitude, 500 nautical miles; initial thrust-weight ratio, 5.0×10^{-6} ; tangential thrusting in plane perpendicular to sunline.

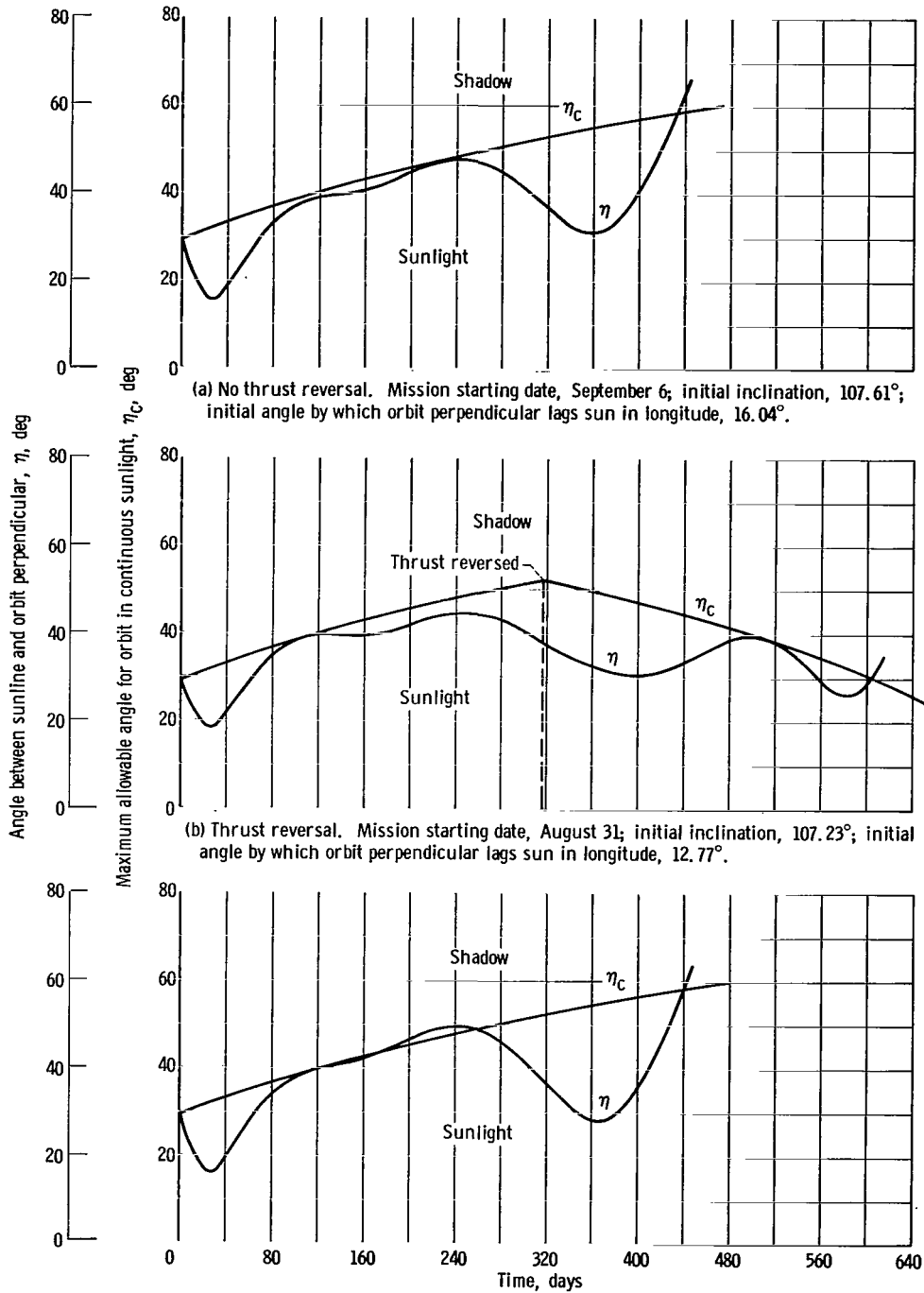
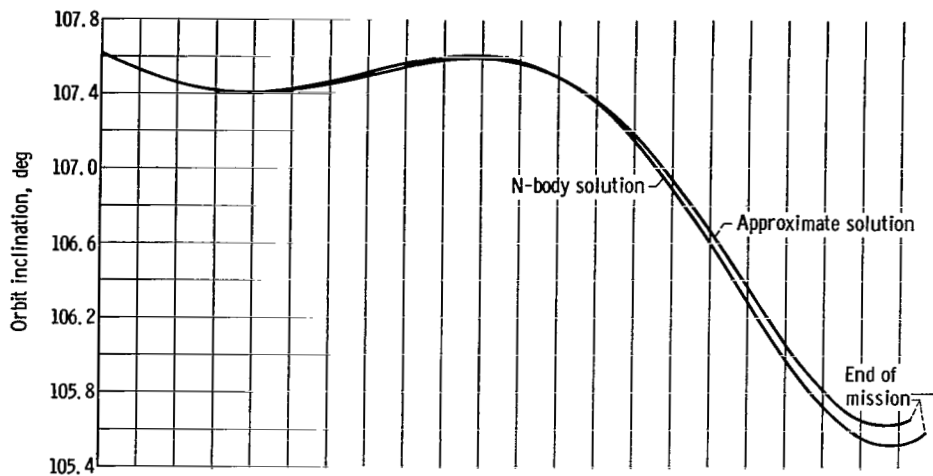
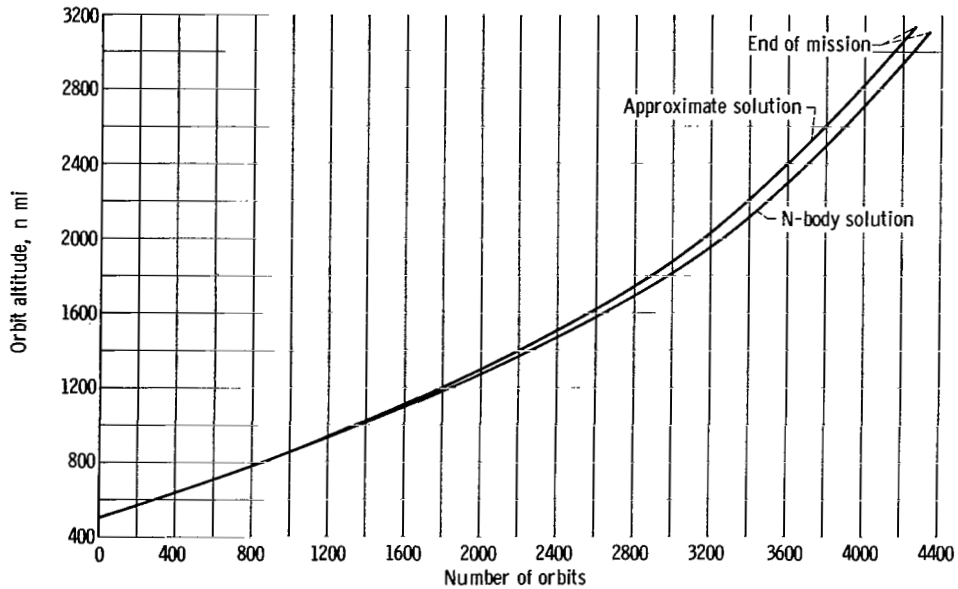


Figure 11. - Comparison of angle between sunline and orbit plane and maximum allowable angle for orbit in continuous sunlight for typical missions. Initial altitude, 500 nautical miles; initial thrust-weight ratio, 5.0×10^{-6} ; orbit index, +1.

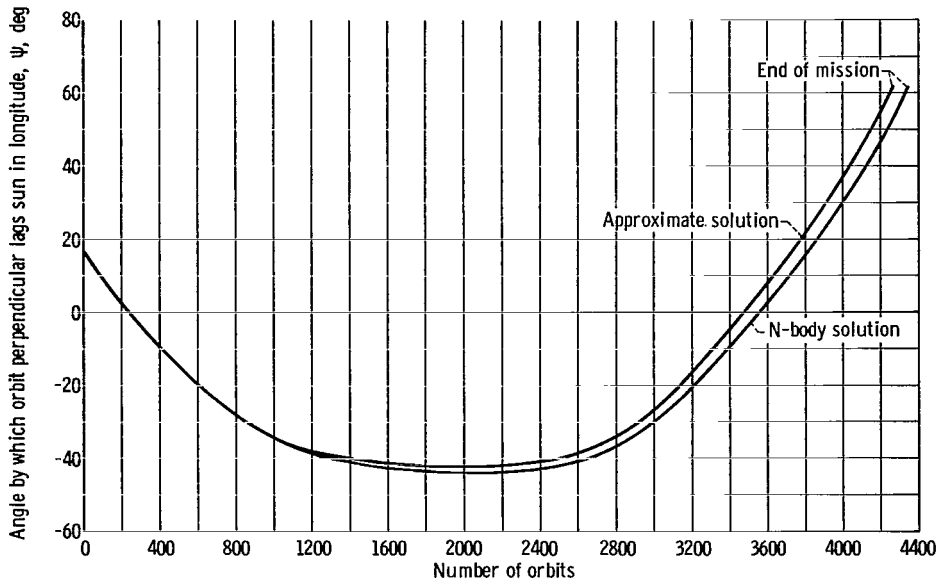


(a) Orbit inclination as function of number of orbits traversed for typical mission in continuous sunlight.



(b) Orbit altitude as function of number of orbits traversed for typical mission in continuous sunlight.

Figure 12. - Comparison of approximate solutions with N-body solution both as function of number of orbits traversed. No thrust reversal; initial altitude, 500 nautical miles; initial thrust-weight ratio, 5.0×10^{-6} ; orbit index, +1; mission starting date, September 6; initial angle by which orbit perpendicular lags sun in longitude, 16.04° ; initial inclination, 107.61° .



(c) Angle by which orbit perpendicular lags sun in longitude as function of number of orbits traversed for typical mission in continuous sunlight.

Figure 12. - Concluded.

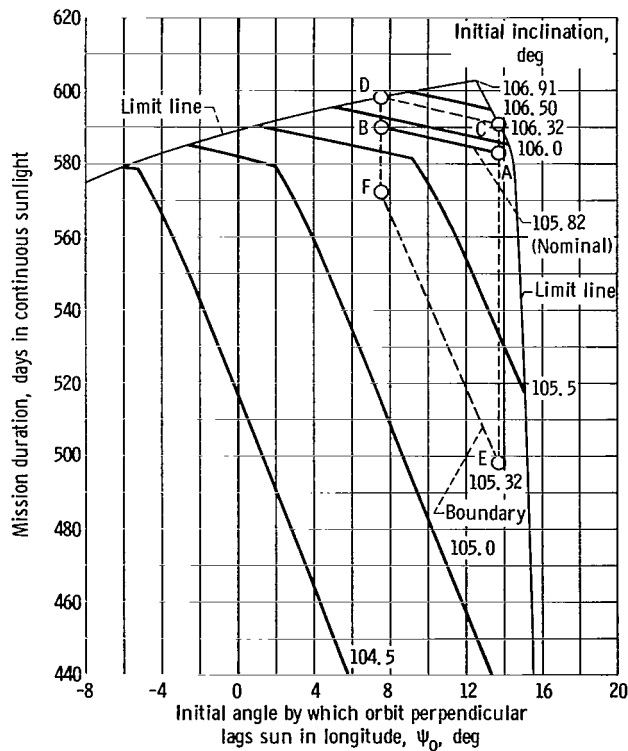


Figure 13. - Mission duration as function of initial angle by which orbit perpendicular lags sun in longitude. Thrust reversal; initial altitude, 485 nautical miles; initial thrust-weight ratio, 5.0×10^{-6} ; mission starting date, August 31; orbit index, +1. (Letters denote discrete points at opening and closing of launch window.)

"The aeronautical and space activities of the United States shall be conducted so as to contribute . . . to the expansion of human knowledge of phenomena in the atmosphere and space. The Administration shall provide for the widest practicable and appropriate dissemination of information concerning its activities and the results thereof."

—NATIONAL AERONAUTICS AND SPACE ACT OF 1958

NASA SCIENTIFIC AND TECHNICAL PUBLICATIONS

TECHNICAL REPORTS: Scientific and technical information considered important, complete, and a lasting contribution to existing knowledge.

TECHNICAL NOTES: Information less broad in scope but nevertheless of importance as a contribution to existing knowledge.

TECHNICAL MEMORANDUMS: Information receiving limited distribution because of preliminary data, security classification, or other reasons.

CONTRACTOR REPORTS: Scientific and technical information generated under a NASA contract or grant and considered an important contribution to existing knowledge.

TECHNICAL TRANSLATIONS: Information published in a foreign language considered to merit NASA distribution in English.

SPECIAL PUBLICATIONS: Information derived from or of value to NASA activities. Publications include conference proceedings, monographs, data compilations, handbooks, sourcebooks, and special bibliographies.

TECHNOLOGY UTILIZATION PUBLICATIONS: Information on technology used by NASA that may be of particular interest in commercial and other non-aerospace applications. Publications include Tech Briefs, Technology Utilization Reports and Notes, and Technology Surveys.

Details on the availability of these publications may be obtained from:

SCIENTIFIC AND TECHNICAL INFORMATION DIVISION
NATIONAL AERONAUTICS AND SPACE ADMINISTRATION

Washington, D.C. 20546